Finite Element Method studies on the stability behavior of cylindrical shells under axial and radial uniform and non-uniform loads

made in

Department of Mechanical and Process Engineering Hochschule Niederrhein

presented by

Myriam Iturgaiz Elso

Matr.-Nr.:868700

Supervising Professor: Prof. Dr. Ing. Conrad Eller

Krefeld, May 2012

Summary of the Final Project Work

Project Title: Finite Element Method studies on the stability behavior of cylindrical shells under axial and radial uniform and non-uniform loads.

Author of the project: Myriam Iturgaiz Elso

Matr.-Nr.: 868700

Supervising professor: Prof. Dr. Ing. Conrad Eller

Supervising organization: Hochschule Niederrhein

Summary of the project: With the help of FEM and ANSYS, the influence of different patterns of axial and radial load was tested on the structural behavior of cylindrical shells. First, the theoretical concepts concerning cylindrical shells are described. The results of stability analysis were shown in the form of graphs, charts and diagrams.

Keywords on the topic: FEM, stability analysis, buckling analysis, ANSYS

Submission of project: May 2012

Affidavit:

I certify by my signature that this final project work was written solely by me.

There were no uses other than those specified by my sources and resources.

The project consists of 87 Pages (without attachments).

Krefeld, in April 2012

(Student's signature)

Preface

At this point I would like to thank all those who were helpful to me during the preparation of project.

I wish to express my sincerest thanks to Prof. Dr. Ing. Conrad Eller for his willingness and consistent support, which was very helpful during the development of this project.

INDEX OF CONTENTS

1. INTRODUCTION

The aim of this project is to analyze the buckling strength of thin cylindrical shells subjected to uniform and non-uniform axial and radial compressive loads.

1.1. Motivation

It is well known that thin cylindrical shell structures have wide applications as one of the important structural elements in many engineering fields. Moreover, its load carrying capacity is decided by its buckling strength which depends strongly on geometrical imperfections presented in it.

Thin cylindrical shell structures are in general highly efficient structures and they have wide applications in the field of mechanical, civil, aerospace, marine, power plants, petrochemical industries, etc. The thin cylindrical shell structures are prone to a large number of imperfections, due to their manufacturing difficulties. These imperfections affect the load carrying capacity of these shells. Reliable prediction of buckling strength of these structures is important, because the buckling failure is catastrophic in nature. That is the reason why the stability tests are increasing and more and more engineers are being asked for the necessary skills to perform calculations in a more accurate way.

Moreover, cylindrical shells used in civil engineering applications are often subjected to very non-uniform axial compressive stresses, but very little research has been conducted on the failure criteria to which they should be designed. Furthermore, cylinders under uniform radial compression have been widely studied, but non-uniform loading has received much less attention. Wind loaded cylinders, which develop non-uniform radial compression have also received some attention, but very limited information exists on the buckling, nonlinear and post-buckling behavior to more general patterns of non-uniform compressive stress.

1.2. Task and procedure

The themes of this thesis are:

- Finite Element Method studies on the stability behavior of cylindrical shells under external uniform and non-uniform axial load.
- Finite Element Method studies on the stability behavior of cylindrical shells under external uniform and non-uniform radial load.

The present work deals with the stability analysis of thin-walled cylindrical shells, with different combinations of loads. It examines how the variable external loads affect the deformation of a cylindrical shell.

The application of thin-walled cylindrical shells, as the essential structural members, has been widely studied by engineers, due to their importance in modern industries. These structures are prone to fail by buckling under external pressure, either axial or radial, which could happen during discharging or wind load. Buckling phenomena occur when most of the strain energy, which is stored as membrane energy, can be converted to bending energy requiring large deformation resulting in catastrophic failure.

The analysis of the different models will be developed with the finite element program ANSYS.

1.3. Literature review

Because of the tremendous and continuous interest in shell buckling and the multitude of reported theoretical and experimental investigations, reviews and surveys have appeared in the open literature since the 1950s.

The first theoretical investigations on the subject dealt with axially loaded configurations, and they were performed by Lorenz, Timoshenko and Southwell. The first experimental studies are those of Lilly, Robertson, Flugge, Lundquist and Donnell. The initial theoretical investigations were based on many simplifying assumptions, and they reduced the mathematical model to a

linear Eigen-boundary-value problem (classical bifurcation approach).

Comparison between theoretical predictions (critical loads) and experimental results (buckling loads) revealed discrepancy of unacceptable magnitude. A tremendous effort was made in order to explain the discrepancy both analytically and experimentally. From the analytical point of view, the initial simplifying assumptions were later reevaluated and removed. This led to studies which attempted to attribute the discrepancy to different factors such as the effects of pre-buckling deformations, in-plane boundary conditions, or initial geometric imperfections.

Initially, the imperfection sensitivity of the system was established through strict post-buckling analyses of the perfect configuration. In addition, some of these investigators explained that the minimum post-buckling equilibrium load is a measure of the load carrying capacity of the system. This thinking came to an end when Hoff, Madsen, and Mayers concluded from their calculations that the minimum post-buckling load tends towards zero with increasing number of terms in the series expansion and with diminishing thickness.

Another approach for imperfection sensitivity studies is to deal directly with the imperfect configuration and employ nonlinear kinematic relations. The first attempt is Donnell's. Koiter was the first to question the use of the minimal post-buckling load as a measure of the load carrying capacity. He also dealt directly with the imperfect configuration. His theory is limited to the neighborhood of the classical bifurcation load (immediate post-buckling), and therefore to small initial imperfections. Many researchers adopted this approach. The single and most important conclusion of all the theoretical investigations of cylindrical shells is that the primary reason for the discrepancy between (linear) theoretical critical loads and buckling loads is that the system is extremely sensitive to initial geometric imperfections.

In parallel to the above analytical investigations, many experimental studies were performed with the same objective in mind. While the old buckling loads fell in the range of 15-50% of the classical critical load, the new ones, with use of carefully manufactured specimens, fall in the range of 40-90% of the classical critical load. Moreover, Thielemann and Esslinger extended their research to include theoretical post-buckled state calculations on the basis of observed experimental results.

A similar development was followed for the case of buckling under lateral loading (pressure).

The first analysis is attributed to von Mises. Several investigations based on linear analyses appear in the literature. Batdorf used simplified Donnell-type of shell equations to predict critical loads. Soong employed Sanders' shell theory. Simitses and Aswani compared critical loads for the entire range of radius to thickness and length to radius ratios and for various load behaviors during the buckling process (true pressure, constant directional pressure, and centrally directed pressure) for a thin cylindrical shell, employing several linear shell theories: Koiter-Budiansky, Sanders, Flugge, and Donnell. Sobe studied the effect of boundary conditions on the critical pressure.

Post-buckling and imperfection sensitivity analyses appear in the literature, as in the case of axial compression. These studies follow the same pattern and include strictly post-buckling analyses, and Koiter-type of analyses. Orthotropic, stiffened, and other constructions were considered by several researchers, including Becker and Gerard, Meek, Hutchinson and Amazigo, Sheinman, and Giri.

Buckling analyses for torsion started with the work of Donnell. Several studies followed with the emphasis on different considerations. Hayashi dealt with orthotropic cylinders, and Lundquist and Nash are two of several that reported experimental results. Hayashi Hirano and Budiansky are among those who reported on post-buckling analyses.

Furthermore, cylindrical shells used in civil engineering applications are often subject to very non-uniform axial compressive stresses (Rotter, 1985, 1998), but very little research has been conducted on the failure criteria to which they should be designed. Most of the existing relevant work examined only the linear bifurcation buckling behavior of a perfect shell (Teng, 1996; Teng and Rotter, 2004). Many civil engineering shells (silos, tanks and digesters) are very thin, so the design is controlled by elastic buckling. Cylinders under uniform axial compression have been widely studied, but non-uniform axial loading has received much less attention. Cylinders under global bending have received some study (Lundquist, 1935; Flügge, 1973; Seide and Weingarten, 1961; Stephens and Starnes, 1975; Antoine, 2000), but the circumferential variation of membrane stress is so slow that the behavior is rather similar to that under uniform compression.

Wind loaded cylinders, which develop non-uniform radial compression have also received some attention (Greiner and Derler, 1995), but very limited information exists on the buckling,

nonlinear and post-buckling behavior of imperfect cylindrical shells subject to more general patterns of non-uniform axial compressive stress (Libai and Durban, 1977; Peter, 1974; Saal, 1982; Rotter, 1985; Cai et al., 2002). Some studies of the load-carrying capacity of column-supported shells have recently been undertaken (e.g. Guggenberger et al., 2000), but these relate to failure above supports rather than buckling within the shell. The studies of Cai et al. (2002, 2003) used similar analyses to explore a problem under different patterns of non-uniform axial compression.

The failure of wind-loaded cantilever cylinders has been reported and investigated since the 1960s.For example, the collapse of oil-storage tanks in England in 1967 was reported by Kundurpi et al. (1975), but failures of this kind have also occurred in many other areas of the world that are subject to high wind conditions without being reported in the open literature. Pressure coefficients for tanks with dome roof (Maher 1966) or flat roof (Purdy et al. 1967) were reported from wind tunnel experiments in the 1960s. A fine set of wind tunnel experiments was done by Johns and co-workers during the 1970s (Kundurpi et al. 1975), who tested small scale cylinders with $1<L/R<5$ and $376<R/t<555$. Resinger and Greiner (1982), Uematsu and Uchiyama (1985), and Megson et al. (1987) reported other tests on cylinders carried out in wind tunnel facilities. Schmidt et al. (1998) published post-buckling results from tests on PVC and steel cylinders under internal suction, and also under a static simulation of wind by means of a pressure that varies over segments of the shell; all cylinders included ring stiffeners on top, except for one case with $L/R = 1$ and $R/t = 2500$, which was tested under internal pressure.

2. DEFORMATIONS AND STRESSES OF CYLINDERS

2.1. Introduction

Depending on the type of material, size, geometry of an object and forces applied, various types of deformation may result:

1. Elastic Deformation

   This type of deformation is reversible. Once the forces are no longer applied, the object returns to its original shape. Linear elastic deformation is governed by Hooke's law, which states:

$$\sigma = E\varepsilon$$

   where σ is the stress, ε indicates the resulting strain and E is a material constant called Young´s modulus. This relationship only applies in the elastic range and indicates that the slope of the stress vs. strain curve can be used to find Young's modulus. The elastic range ends when the material reaches its yield strength. At this point plastic deformation begins.

2. Plastic Deformation

   This type of deformation is irreversible. Two different phases can occurred during the plastic deformation:

   - Strain hardening: The material becomes stronger through the movement of atomic dislocations.
   - Necking: It is indicated by a reduction in cross-sectional area of the structure. Necking begins after the ultimate strength is reached. During necking, the material can no longer withstand the maximum stress and the strain rapidly increases. Plastic deformation ends with the fracture of the material.

That can be checked in the strain-stress graphic, which provide a huge amount of information.

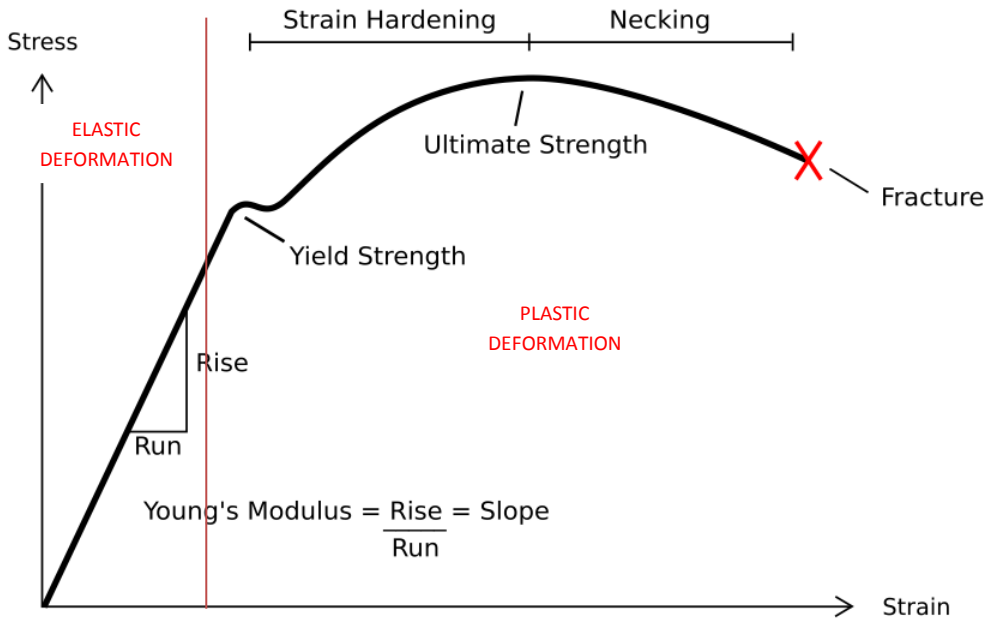

Figure 1: Stress vs. Strain

2.2. Thin-walled Cylinders

2.2.1. Stresses

The stresses in thin-walled cylinders have been wide studied, due to the huge amount of applications that they have, such as boiler shells, pressure tanks, pipes…

Generally three types of stresses are developed in pressure shells:

- Circumferential or ring stresses ($\boldsymbol{\sigma_\theta}$)
- Longitudinal or axial stresses ($\boldsymbol{\sigma_L}$)
- Radial stresses ($\boldsymbol{\sigma_r}$)

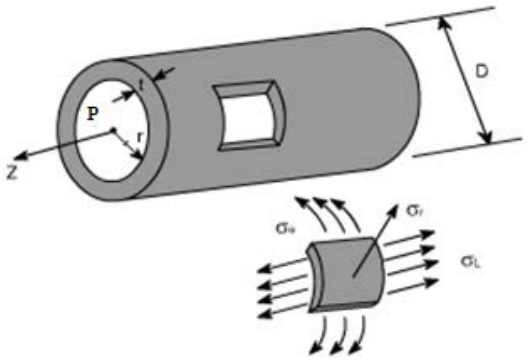

Figure 2: Thin-walled Cylinder under pressure

1. Ring stresses

It is a type of mechanical stress of a cylindrically shaped part as a result of internal or external pressure. It can be defined as the average force exerted circumferentially (perpendicular both to the axis and to the radius) on every particle in the cylinder wall.

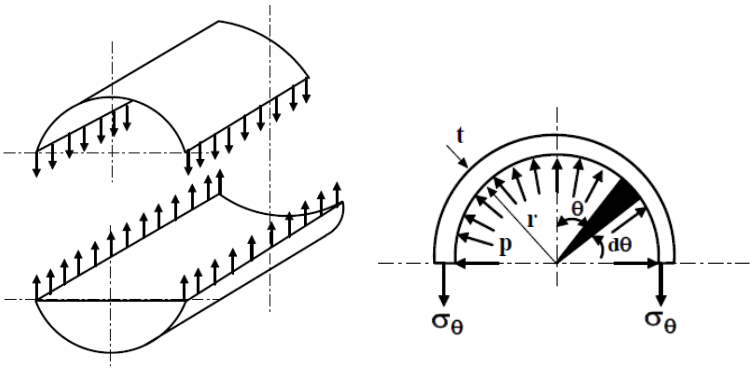

Figure 3: Hoop Stress

So long as the wall thickness is small compared to the diameter then the force trying to split the cylinder due to the pressure is

$$F = 2\int_0^{\frac{\pi}{2}} prL\cos\theta\, d\theta = 2prL = pD_iL$$

The cross-section area which sustains this force is given by

$$\boldsymbol{A = 2tL}$$

Therefore the ring stress is defined by

$$\boldsymbol{\sigma_\theta = \frac{F}{A} = \frac{pD_iL}{2tL} = \frac{pD_i}{2t}}$$

An alternative to ring stress in describing circumferential stresses is wall stress or wall tension (T), which is usually defined as the total circumferential force exerted along the entire radial thickness.

$$\boldsymbol{T = \frac{F}{L}}$$

The classic example of this stress is the tension applied to the iron bands of a wooden barrel.

2. Axial stresses

They are the stresses that occur in the longitudinal direction.

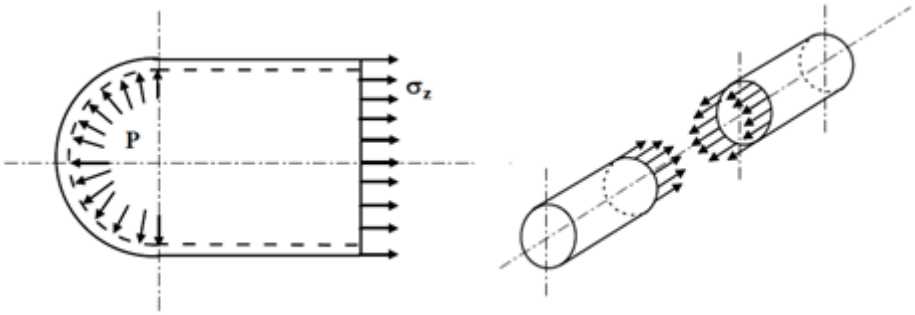

Figure 4: Axial Stress

In this case we consider the forces trying to split the cylinder along the length. The force due to the pressure is

$$F = \int_0^r 2\,p\pi r\,dr = 2p\pi\frac{r^2}{2} = p\frac{\pi {D_i}^2}{4}$$

The cross-section area which sustains the force in this case is given by:

$$A = \pi D_i t$$

This area has been approximated to a rectangle whose dimensions are the length of the circumference (πD_i) and the thickness.

Consequently the axial stress is defined by:

$$\sigma_L = \frac{F}{A} = \frac{p\frac{\pi {D_i}^2}{4}}{\pi D_i t} = \frac{pD_i}{4t}$$

3. Radial stresses

The radial stresses are normal to the curved plane of the isolated element.

In thin-walled cylinder theory, they are normally not considered, because they are neglibly small compared to the other two stresses.

2.2.2 Thin-walled Cylinder Displacement

Consider a small rectangular area which is part of the wall in a thin walled cylinder.

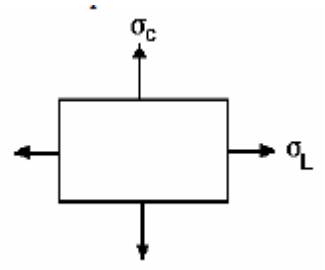

Figure 5: Thin-walled cylinder wall

There are two stresses perpendicular to each other, the axial ($\boldsymbol{\sigma_L}$) and circumferential ($\boldsymbol{\sigma_c}$) stresses, as explained before.

From basic stress and strain theory the corresponding axial strain is:

$$\boldsymbol{\varepsilon_L = \frac{1}{E}(\sigma_L - \mu\sigma_c)}$$

Substituting both stresses with the formulas calculated in the last chapter, the following formula for the longitudinal strain is obtained:

$$\boldsymbol{\varepsilon_L = \frac{\Delta L}{L} = \frac{1}{E}\left(\frac{pD}{4t} - \mu\frac{pD}{2t}\right) = \frac{pD}{4tE}(1 - 2\mu)}$$

The circumferential strain may be defined as follows.

$$\boldsymbol{\varepsilon_c = \frac{change\ in\ circumference}{original\ circumference}}$$

$$\boldsymbol{\varepsilon_c = \frac{\pi(D + \Delta D) - \pi D}{\pi D} = \frac{\Delta D}{D}}$$

The conclusion obtained is that the circumferential stress is the same as the strain based on diameter, in other words, the diametric strain.

From basic stress and strain theory, the corresponding circumferential strain is:

$$\boldsymbol{\varepsilon_c = \frac{1}{E}(\sigma_c - \mu\sigma_L)}$$

Substituting both stresses with the formulas calculated in the last chapter, the following formula for the circumferential strain is obtained:

$$\boldsymbol{\varepsilon_c = \frac{\Delta D}{D} = \frac{1}{E}\left(\frac{pD}{2t} - \mu\frac{pD}{4t}\right) = \frac{pD}{4tE}(2 - \mu)}$$

For defining the volumetric strain, it is necessary to take into account the following parameters:

- **Original Length** $= \mathbf{L_1}$
- **Original cross sectional area** $= \frac{\pi D^2}{4}$
- **Original Volume** $= \frac{\pi D^2}{4} L_1$
- **New Length** $= L_2 = L_1 + \Delta L$
- **New cross sectional area** $= \frac{\pi(D+\Delta D)^2}{4}$
- **New Volume** $= \left(\frac{\pi(D+\Delta D)^2}{4}\right)(L_1 + \Delta L)$

Then, the volumetric strain can be written as

$$\varepsilon_v = \frac{\Delta V}{V} = \frac{\left(\frac{\pi(D+\Delta D)^2}{4}\right)(L_1 + \Delta L) - \left(\frac{\pi D^2}{4}\right)L_1}{\left(\frac{\pi D^2}{4}\right)L_1}$$

Dividing out, clearing brackets and ignoring the product of two small terms, this reduces to

$$\varepsilon_v = \frac{\Delta L}{L_1} + 2\frac{\Delta D}{D} = \varepsilon_L + 2\varepsilon_c$$

Substituting the equations for the axial and circumferential stresses into this, leads to

$$\varepsilon_v = \frac{pD}{4tE}(5 - 4\mu)$$

3. BUCKLING

3.1. Introduction

Buckling is a process by which a structure cannot withstand loads with its original shape, so that it changes its shape in order to find a new equilibrium configuration. It is generally resulting from structural instability due to a compressive action on the element involved. The effects are basically geometric, like large displacements or even plasticity in the walls of the structure.

Different stability theories have been formulated in order to determine the conditions under which a structural system, which is in equilibrium, ceases to be stable. The load for which a structure ceases to be stable and starts to buckle is known as the "Critical Buckling Load" (P_{cr}).

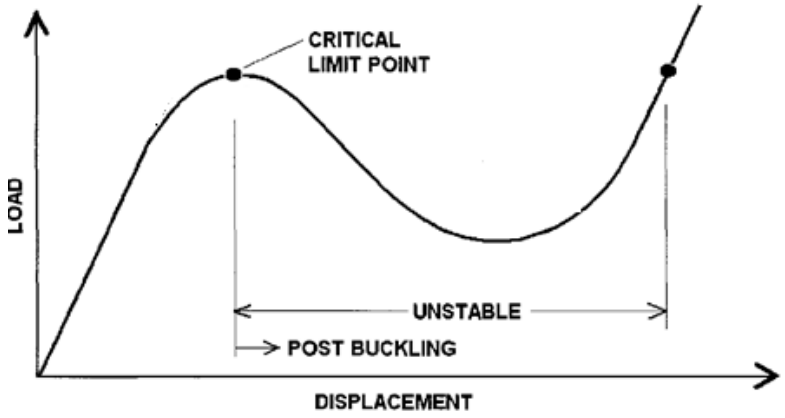

Figure 6: Load deflection diagram

It is a so relevant value in order to analyze the behavior of a structure. Three different types of equilibriums can be reached:

1. Stable equilibrium: The pressure applied doesn´t reach the critical load, so that the structure returns to its original equilibrium state when the force is removed.

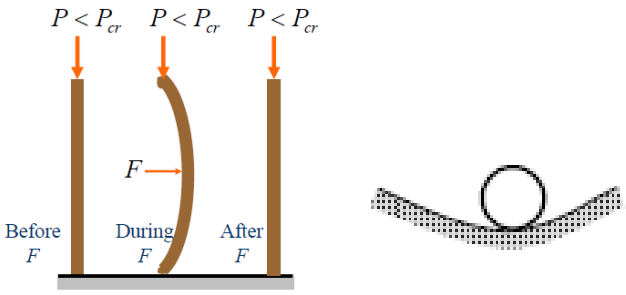

Figure 7: Stable equilibrium

2. Neutral or indifferent equilibrium: The load reached exactly the critical point and the elastic restoring force is not sufficient to return the structure to its initial position.

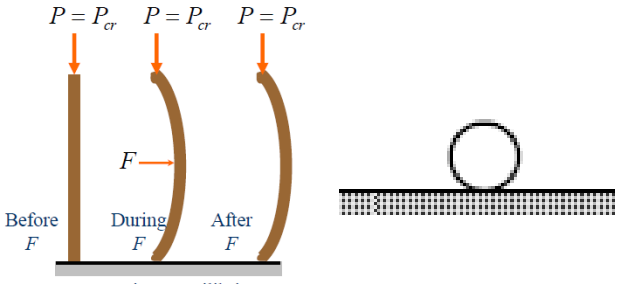

Figure 8: Neutral equilibrium

3. Unstable equilibrium: If the system is subjected to a compressive load that exceeds the critical buckling pressure, the column will bend considerably. Depending on the magnitude of the load, the structure either will remain in the bent position or will completely collapse and fracture.

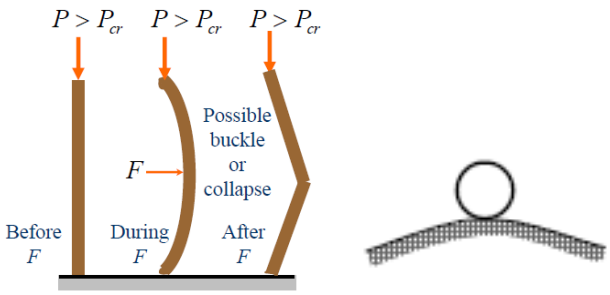

Figure 9: Unstable equilibrium

3.2 Types of Buckling

The way in which buckling occurs depends on how the structure is loaded and on its geometrical and material properties. The pre-buckling process is often non-linear if there is a reasonably large percentage of bending energy being stored in the structure throughout the loading history.

According to the percentage of bending energy, the two basic ways in which a conservative system may lose its stability are: nonlinear or limit point buckling and bifurcation buckling.

3.2.1 Nonlinear collapse

In this way of buckling, the systems initially deform slowly and the stiffness of the structure or the slope of the load-deflection curve, decreases with increasing load. At the critical buckling point, the load-deflection curve has zero slope, and if the load is maintained, failure of the structure is usually dramatic and instantaneous.

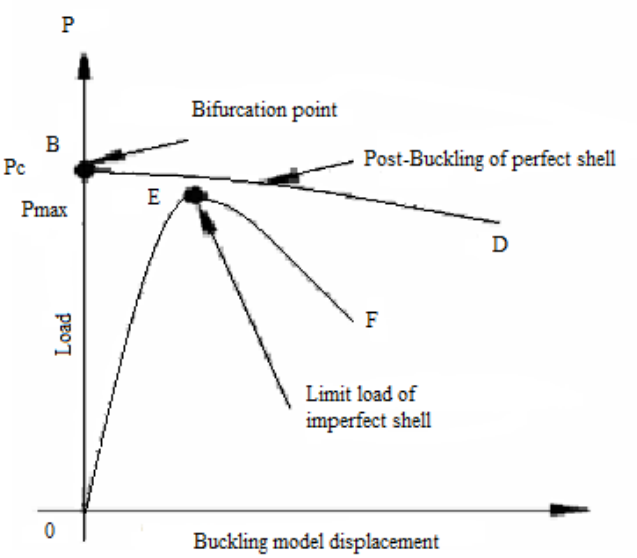

Figure 10: Load deflection diagram: Nonlinear buckling

3.2.2. Bifurcation Buckling

It refers to a different kind of failure. At the bifurcation point (critical load is reached), where the primary and secondary paths intersect, more than one equilibrium position is possible. The primary path is not usually followed after loading exceeds this point and the structure is in the post-buckling state. The slope of the secondary path at the bifurcation point determines the nature of the post-buckling. Positive slope indicates that the structure will have post buckling strength, whilst a negative slope means that the structure will simply collapse.

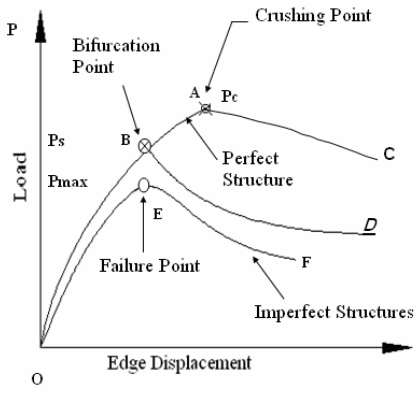

Figure 11: Load deflection diagram: Bifurcation buckling

3.3. Post-buckling of perfect and imperfect systems

After the bifurcation point, three main situations can happen depending on the type of system under study.

1. Stable-symmetric point of bifurcation: The buckling is characterized by a quick growth of the deflections after the critical point of the perfect system is reached.

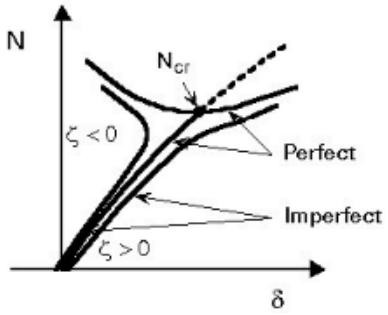

Figure 12: Stable-symmetric point of bifurcation

After the bifurcation, the load can be increased, that means the structure has a stable behavior after buckling. It is a common case of post-buckling in columns, beams and plates.

2. Unstable-symmetric point of bifurcation: After reaching the bifurcation load the structure collapses immediately. Imperfections play a more important role that in the case before. Small imperfections can have a huge influence reducing the critical load.

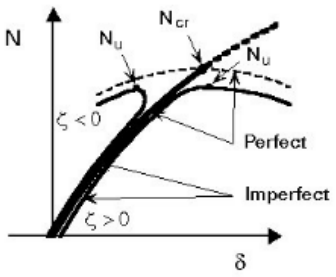

Figure 13: Unstable-symmetric point of bifurcation

3. Asymmetric point of bifurcation: Depending on the direction of the imperfection, a symmetric stable or an asymmetric unstable behavior results. It is the extreme case, because the system loses its stability at a limit point (quite reduced comparing to the critical point) for small positive values of the imperfection.

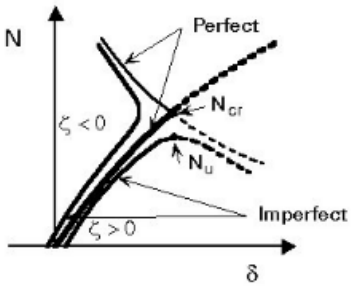

Figure 14: Asymmetric point of bifurcation

3.4. Buckling of thin cylindrical shells

As commented before, thin-walled shells have many applications in engineering such as underground pipes and outer shells of submarines. When designing those structures one should consider not only the strength problem in service, but also the buckling problem. They are prone to a large number of imperfections, due to their manufacturing difficulties.

These imperfections affect the load carrying capacity of these shells. The imperfections that affect the strength of thin cylindrical shells are classified into three main groups:

1. Geometrical: Out-of straightness, initial ovality and geometrical eccentricities.
2. Structural: Small holes, residual stresses and material inhomogenities.
3. Loading imperfections: Imperfect boundary conditions, non-uniform edge load distribution, load eccentricities.

The differential equation of the classical buckling theory of a thin-walled shell is written as

$$\frac{D}{h}\nabla^8 w + Ek_x^2\frac{\partial^4 w}{\partial y^4} + 2Ek_x k_y\frac{\partial^4 w}{\partial x^2 \partial y^2} + Ek_y^2\frac{\partial^4 w}{\partial x^4} - \sigma_x^{(0)}\nabla^4\left(\frac{\partial^2 w}{\partial x^2}\right) - 2\sigma_{xy}^{(0)}\nabla^4\left(\frac{\partial^2 w}{\partial x \partial y}\right) - -\sigma_y^{(0)}\nabla^4\left(\frac{\partial^2 w}{\partial y^2}\right) = 0$$

where $\sigma_x^{(0)}, \sigma_{xy}^{(0)}, \sigma_y^{(0)}$ are the initial membrane stresses; w is buckling deflection in the z direction; E is Young´s modulus; μ is the Poisson´s ratio; h and L are, respectively thickness and length of the shell; $D = \frac{Eh^3}{[12(1-\mu^2)]}$ is the bending stiffness; k_x, k_y , curvature in x ,y direction.

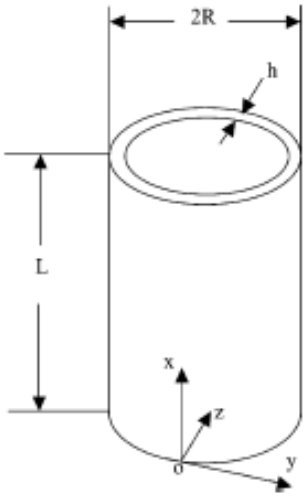

Figure 15: Structure of a thin-walled shell and its coordinate system

3.5. Buckling of thin-walled cylinders under axial pressure

3.5.1. Introduction

Thin-walled cylindrical shells are, in general, highly efficient structures; and they have wide practical application, for example, in the aerospace, petrochemical and construction industries. When thin-walled shell structures are loaded in compression, their strength is limited by buckling; and since such buckling is often catastrophic, reliable prediction of the buckling strength of shells is a strong aspiration of engineers.

In addition to this, cylindrical shells used in civil engineering applications are often subject to very non-uniform axial compressive stresses, but very little research has been conducted on the failure criteria to which they should be designed. Cylinders under uniform axial

compression have been widely studied, but non-uniform axial loading has received much less attention. Wind loaded cylinders, which develop non-uniform radial compression have also received some attention, but very limited information exists on the buckling, nonlinear and post-buckling behavior to more general patterns of non-uniform axial compressive stress.

Therefore, the present section is concerned with aspects of the elastic buckling of thin cylindrical shells under uniform and non-uniform axial compression.

3.5.2. Ways of solving the buckling problem

3.5.2.1. Analytic Solution

If a cylindrical shell simply supported at the ends is uniformly compressed in the axial direction as shown in Fig. 16, the general solution for very small displacements can be given in the following form[1]:

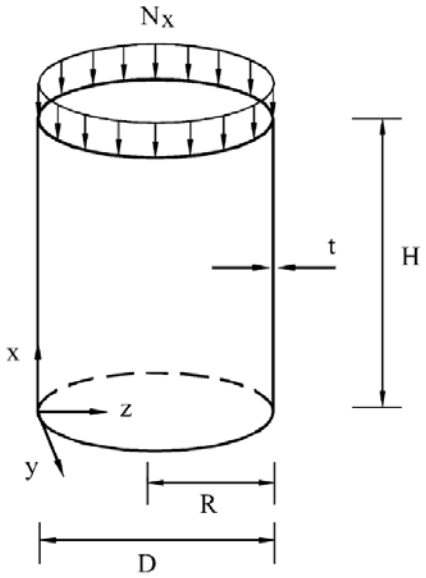

Figure 16: Cylindrical shell subjected to axial load

[1] Subtracted from the article "Buckling strength of the cylindrical shell and tank subjected to axially compressive loads"; Seung-Eock Kim, Chang-Sung Kim

$$u = A\sin(n\theta)\cos\left(\frac{m\pi x}{H}\right), \quad (1)$$

$$v = B\sin(n\theta)\cos\left(\frac{m\pi}{H}\right), \quad (2)$$

and

$$w = \mathrm{C}\sin(\mathrm{n}\theta)\cos\left(\frac{\mathrm{m}\pi}{\mathrm{H}}\right) \quad (3)$$

where *A*, *B* and *C* are constants; *H* is the height of the cylindrical shell; and *n* and *m* are the buckling number of circumferential and longitudinal half-waves, respectively. When the simply supported conditions of $w = 0$ and $d^2w/dx^2 = 0$ are used at the ends, the critical stress is obtained as

$$\sigma_{cr} = \frac{N_x}{t} = \frac{R\,E}{S(1-\nu^2)}, \quad (4)$$

$$R = (1-\nu^2)\lambda^4 + \alpha[(n^2+\lambda^2)^4 - (2+\nu)(3-\nu)\lambda^4 n^2 + 2\lambda^4(1-\nu^2) - \lambda^2 n^4(7+\nu) + \lambda^2 n^2(3+\nu) + n^4 - 2n^6],$$

$$S = \lambda^2\left\{(n^2+\lambda^2)^2 + \frac{2}{1-\nu}\left(\lambda^2 + \frac{1-\nu}{2}n^2\right)[1+\alpha(n^2+\lambda^2)^2] - \frac{2\nu^2\lambda^2}{1-\nu} + \frac{2\alpha}{1-\nu}\left(\lambda^2 + \frac{1-\nu}{2}n^2\right)[n^2 + (1-\nu)\lambda^2]\right\},$$

$$\alpha = \frac{t^2}{12R^2},$$

$$\lambda = \frac{mR\pi}{H},$$

N_x is the axial force, E is Young's modulus, ν is Poisson's ratio, t is the thickness of the shell, and R is the radius of the shell. Theoretically, the critical stress of Eq. (4) has an infinite number of solutions as the values of *m* and *n* vary. The minimum critical stress among these is determined as the buckling stress. One difficulty in using Eq. (4) is that the *m* and *n* values leading to the buckling stress are unknown until a large number of critical stresses are calculated and compared. As a result, the equation essentially requires a lot of calculations of critical stresses depending on the values of m and n in order to get the lowest critical stress,

i.e. buckling stress.

Assuming that many buckling waves (m) form along the length of the cylinder, the value of λ^2 becomes large. Then, Eq. (4) can be simplified in the following form:

$$\sigma_{cr} = \frac{N_x}{t} = \frac{1-\nu^2}{E}\left(\alpha\frac{(n^2+\lambda^2)^2}{\lambda^2} + \frac{(1-\nu^2)\lambda^2}{(n^2+\lambda^2)^2}\right) \quad (5)$$

When the value of *n* in Eq. (5) is equal to zero, axisymmetric buckling occurs, and Eq. (5) is simplified as

$$\sigma_{cr} = \frac{N_x}{t} = D\left(\frac{m^2\pi^2}{tH^2} + \frac{EH^2}{R^2Dm^2\pi^2}\right) \quad (6)$$

where $\mathrm{D} = \mathrm{Et}^3/[12(1-\nu^2)]$ is the flexural rigidity. Since σ_{cr} is a continuous function of $\mathrm{m}\pi/\mathrm{H}$, the minimum value of Eq. (6) can be written in the following form:

$$\boldsymbol{\sigma_{cr} = \frac{Et}{R\sqrt{3(1-\nu^2)}}} \quad (7)$$

where *E* is Young´s Modulus, *t* is the shell thickness, *R* is the shell radius, ν is Poisson's ratio.

Furthermore, it is possible to see that the classical buckling stress doesn´t depend on the buckling form. This calculation is valid only for purely axially loaded isotropic cylinders with traditional bearing.

Applying the classical buckling stress to this work, the determination of a linear critical load is required, so the σ_{cr} will be multiplied by the thickness of the cylindrical shell in order to obtain a result in N/mm.

3.6. Buckling of thin-walled cylinders under radial pressure

3.6.1. Introduction

The stability of circular cylindrical shells under uniform lateral pressure has been widely investigated. The behavior of cylindrical shells under external pressure is quite sensitive to geometric imperfections. There have been many theoretical studies investigating the strength of cylinders with specific imperfection forms, and it is well established that axisymmetric imperfections cause the greatest reductions in the buckling strength.

When thin shells are subjected to external pressure, the collapse is initiated by yielding, which is often the dominant factor, while the interaction with the instability is meaningful. In fact, the presence of imperfections reduces the load bearing capacity, so the classical elastic solution appears to be not adequate.

The major factors that affect the collapse pressure of thin-walled cylinders are the diameter-to-thickness ratio D/t, the Young's modulus and yield stress of the material in the circumferential direction, and initial imperfections in the form of ovality and wall thickness variations.

3.6.2. Ways of solving the buckling problem

3.6.2.1. Analytic Solution

There are a lot of different analytic solutions for thin-walled cylinders under external pressure, depending on the characteristics of the cylinder and the constraints applied.

Considering a **single-wave buckling mode**, Glock calculated a solution of the buckling problem of **constrained elastic cylinders**. Glock used energy formulation in order to obtain the formula of the critical buckling load.

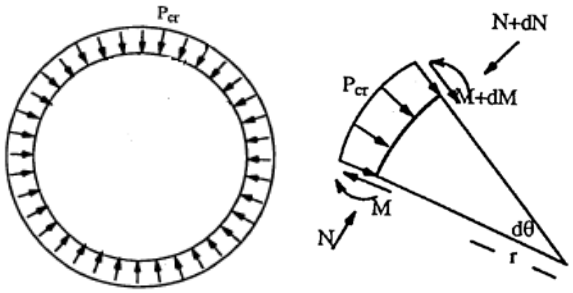

Figure 17: Glock´s Model Section

According to the Glock´s approach, the deflection is described by the following equation[2]:

$$w = w_1 \, sin^2\left(\frac{\pi\theta_v}{2\theta}\right)$$

where w = deflection of the buckled area

w_1 = deflection amplitude in the buckling area

θ_v = variable of angle

θ = angle of the buckling area

As the cylinder buckles, the potential energy includes three parts:

1. Flexural moment M within the buckling region.
2. Ring compressive force N
3. External uniform pressure P_{cr} accumulated during the process.

Combining these parts, the following expression can be obtained:

$$\Pi = \frac{1}{2}\frac{EI}{r^3} \int_0^{\theta_o} (w + \ddot{w})^2 \, d\theta + \int_0^{\pi} \frac{N^2}{2EF} r \, d\theta - \int_0^{\theta_o} (w + \ddot{w})^2 \int_0^{\theta_o} P_{cr} \, w r d\theta$$

[2] Subtracted from the article "Buckling Models and Influencing Factors for Pipe Rehabilitation Design"; Leslie K. Guice and J.Y. Li

where Π = potential energy

EI = flexural stiffness of the thin cylinder

EF = tensile stiffness of the thin ring

N = hoop compressive force

After substituting and integrating the equation above, the potential energy may be written as

$$\Pi = \frac{1}{16}\frac{EI}{r^3}\left(\frac{\pi}{\theta}\right)^4 {w_1}^4\,\theta + \frac{N^2}{2}\frac{r\pi}{EF} - \frac{P_{cr}r}{2}w_1\theta$$

The minimum potential energy criterion should satisfy the following requirements:

$$\frac{\delta\Pi}{\delta w_1} = \frac{1}{4}\frac{EI}{r^3}\theta\left(\frac{\pi}{\theta}\right)^4 {w_1}^3 + N\frac{\delta N}{\delta w_1}\frac{r\pi}{EF} - \frac{P_{cr}}{2}r\theta = 0$$

$$\frac{\delta^2\Pi}{\delta w_1^2} = \frac{3}{4}\frac{EI}{r^3}\theta\left(\frac{\pi}{\theta}\right)^4 {w_1}^2 + \left[\left(\frac{\delta N}{\delta w_1}\right)^2 + N\left(\frac{\delta^2 N}{\delta {w_1}^2}\right)\right]\frac{r\pi}{EF} = 0$$

Solving both equations simultaneously, the following equation for the critical external pressure is reached:

$$\left(\frac{P_{cr}r^3}{EI}\right)_{cr} = 0.969\left(\frac{r^2EF}{EI}\right)^{\frac{2}{5}}$$

That equation is the result of Glock´s approach, but if the assumption is made that the flexural modulus of elasticity is approximately equal to the tensile modulus and considering the condition of plane-strain, the equation can be simplified as:

$$p_{cr} = \frac{E}{1-\nu^2}\left(\frac{t}{D}\right)^{2,2}$$

where E is the Young's modulus, ν the Poisson's ratio, D the cylinder diameter, and t the wall thickness.

Moreover, considering a single-wave buckling mode for **long (free of boundary conditions)** perfectly round elastic cylinders, the value of the critical pressure is given by the following formula:

$$p_{GL} = \frac{E}{1-\mu^2}\left(\frac{t}{D}\right)^3$$

This applies for cylinder lengths that fit:

$$L > \frac{4\pi\sqrt{6}}{27}(1-\mu^2)^{0.25} d\sqrt{\frac{d}{t}}$$

If a cylinder does not fall into that "long" category above the last equation is not suitable. There are two equations for short cylinders, of which the Von Mises is considered the better.

The first one is the Southwell equation. It only takes radial pressure into account (not axial) and the critical buckling pressure is

$$p_c = \frac{1}{3}(n^2-1)\frac{2E}{1-\mu^2}\left[\frac{t}{d}\right]^3 + \frac{2E\frac{t}{d}}{(n^2-1)n^4\left[\frac{2L}{\pi d}\right]^4}$$

where n in the number of waves in circumferential direction at collapse.

The second equation is called Von Mises equation. It may be used for cylinders subject to combined radial and axial pressure, or just radial. The critical pressure is

$$P_C = \frac{1}{n^2-1+\left(\frac{\pi d}{8L}\right)^2}\left[\left(\left[n^2+\left(\frac{\pi d}{2L}\right)^2\right]^2 - 2k_1n^2 + k_2\right) * \frac{1}{3}\frac{2E}{1-\mu^2}\left(\frac{t}{d}\right)^3 + \frac{\frac{2Et}{d}}{\left[\left(\frac{2nL}{\pi d}\right)^2+1\right]^2}\right]$$

where

$$k_1 = (1 + (1 + \mu)\rho)(2 + (1 - \mu)\rho)$$

$$k_2 = [1 - \rho\mu]\left[1 + \rho(1 + 2\mu) - \mu^2(1 - \mu^2)\left(1 + \frac{1 + \mu}{1 - \mu}\rho\right)\right]$$

and

$$\rho = \frac{1}{\left(\frac{2nL}{\pi d}\right)^2 + 1}$$

For both Von Mises and Southwell equations, n is the number of buckling waves, t the wall thickness, d the diameter of the cylinder, μ the Poisson´s ratio and L the length of the cylinder.

3.6.2.2. Weighted Method Solution

Theoretical method can only solve some relatively simple problems. However, for more complicated problems it leads to a very complicated form such as an exponential series solution or a Fourier series solution. The weighted method is a really useful tool for solving complicated buckling problems by making use of the solutions of special simple problems. To determine the weights, some special known results are applied.

As mentioned before, the differential equation of the classical buckling theory of a thin-walled shell is

$$\frac{D}{h}\nabla^8 w + Ek_x^2\frac{\partial^4 w}{\partial y^4} + 2Ek_x k_y\frac{\partial^4 w}{\partial x^2 \partial y^2} + Ek_y^2\frac{\partial^4 w}{\partial x^4} - \sigma_x^{(0)}\nabla^4\left(\frac{\partial^2 w}{\partial x^2}\right) - 2\sigma_{xy}^{(0)}\nabla^4\left(\frac{\partial^2 w}{\partial x \partial y}\right) -$$
$$-\sigma_y^{(0)}\nabla^4\left(\frac{\partial^2 w}{\partial y^2}\right) = 0 \qquad (1)$$

where $\sigma_x^{(0)}, \sigma_{xy}^{(0)}, \sigma_y^{(0)}$ are the initial membrane stresses; w is buckling deflection in the z direction; E is Young´s modulus; μ is the Poisson´s ratio; h and L are, respectively thickness and length of the shell; $D = \frac{Eh^3}{[12(1-\mu^2)]}$ is the bending stiffness; k_x, k_y , curvature in x ,y direction.

In axisymmetric problems $\sigma_{xy}^{(0)} = 0$. Then, applying that to the equation 1, we have

$$\frac{D}{h}\nabla^8 w + Ek_x^2\frac{\partial^4 w}{\partial y^4} + 2Ek_x k_y\frac{\partial^4 w}{\partial x^2 \partial y^2} + Ek_y^2\frac{\partial^4 w}{\partial x^4} - \sigma_x^{(0)}\nabla^4\left(\frac{\partial^2 w}{\partial x^2}\right) - \sigma_y^{(0)}\nabla^4\left(\frac{\partial^2 w}{\partial y^2}\right) = 0 \qquad (2)$$

Because there are no odd partial derivates, variables can be separated so that we can suppose a buckling deflection function that satisfies whose general form is

$$w = f(x)\,sin\frac{ny}{R}$$

where

$$f(x) = \sum_i^m f_i(x)$$

Substituting the last two equations into the equation 2, a series of equations in x is obtained. Assuming that coefficients before the same powers of x are equal zero, there are (m+1) equations for p_0, p_1,p_2,…p_m.

Introducing weights λ_1, λ_2,… λ_m, where, the corresponding solution can be written as

$$p = \sum_i^m \lambda_i p_i$$

What should we do to determine the weights λ_0 ,λ_1, λ_2,… λ_m ?

We can find $\lambda_{i,}$ substituting m groups of known results for p^i_{cr} , n^i (i=1,2,…m) from the finite elements calculations and solving the group of equations. Finally we can substitute n=1,2,3… for different buckling modes into equation 1. The minimum is the desired critical load p_{cr}.

4. FINITE ELEMENT METHOD

4.1. Introduction

The Finite Element Method (FEM) has become very important to solve engineering problems, allowing solving cases that until recent time were virtually impossible by traditional mathematical methods. This required to prototype, test them and make improvements iteratively, what brought high costs both financially and in time of development.

The FEM provides a mathematical model for calculating the real system, easier and cheaper to change than a prototype. However, it remains as an approximate calculating method due to the basic assumptions of the method. Therefore, prototypes are still necessary, but in lower quantity, since the first one can be well approximated to the optimum design.

The finite element method as mathematical formulation is relatively new; although its basic structure has been known for quite a long time, in recent years a great development has been achieved due to the advances in computer technology. These computer advances have allowed the user applying many programs that can perform finite element calculations. Furthermore, FEM allows detailed visualization of where structures bend or twist, and indicates the distribution of stresses and displacements.

The general idea of the finite element method is to divide a continuum in a set of small elements interconnected by a range of points called nodes.

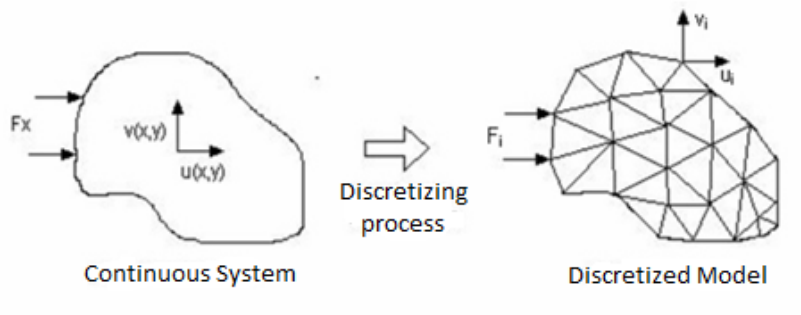

Figure 18: Finite Element Method

The equations governing the behaviour of the continuum also govern the element's behaviour.

In any system subject to analysis, next parts can be distinguished:

- Domain: Geometric space where the system is analysed.
- Boundary conditions: Known variables that determine changes in the system: load, displacement, temperature, voltage, heat sources...
- Unknown factor: System variables to know after the boundary conditions have been applied on the system: displacements, stresses, temperatures...

4.2. How the finite element method works

In a continuum problem of any dimension the field variable (whether it is pressure, temperature, displacement, stress, or some other quantity) possesses infinitely many values because it is a function of each generic point in the body or solution region. Consequently, the problem is one with an infinite number of unknowns.

The finite element discretization procedures reduce the problem to one with a finite number of unknowns by dividing the solution region into elements and by expressing the unknown field variable in terms of assumed approximating functions within each element. The approximating functions (sometimes called interpolation functions) are defined in terms of the values of the field variables at specified points called nodes. In addition to boundary nodes, an element may also have a few interior nodes. The nodal values of the field variable and the interpolation functions for the elements define completely the behaviour of the field variable within the elements.

For the finite element representation of a problem, the nodal values of a field variable become the unknowns. Once these unknowns are found, the interpolation functions define the field variable throughout the assemblage of elements.

Clearly, the nature of the solution and the degree of approximation depend not only on the size and number of the elements used but also on the interpolation functions selected. As one would expect, we cannot choose functions arbitrarily, because certain compatibility conditions should be satisfied. Often functions are chosen so that the field variable or its derivatives are

continuous across adjoining element boundaries. These are applied to the formulation of different kinds of elements.

However, an important feature of the finite element method that sets it apart from other numerical methods has not been mentioned. This feature is the ability to formulate solutions for individual elements before putting them together to represent the entire problem. This means, for example, that if a problem in stress analysis is being treated, the force–displacement or stiffness characteristics of each individual element is found and then the elements are assembled to find the stiffness of the whole structure. In essence, a complex problem reduces to considering a series of greatly simplified problems.

Regardless of the approach used to find the element properties, the solution of a continuum problem by the finite element method always follows an orderly step-by-step process.

To summarize in general terms how the finite element method works, the steps of proceeding are briefly described.

A body of matter (solid, liquid, or gas) or simply a region of space in which a particular phenomenon is occurring is considered.

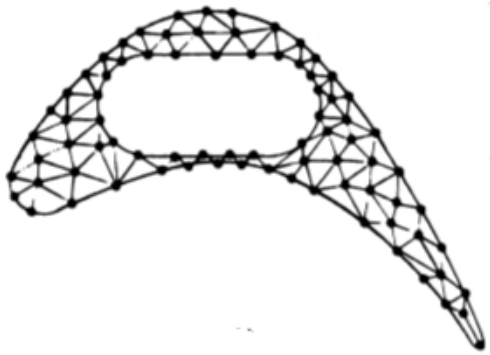

Figure 19: Finite element discretization of a turbine blade profile

The steps to follow in order to perform a finite element method analysis are:

1. **Discretize the Continuum.** The first step is to divide the continuum or solution region into elements. In the example of Figure 17 the turbine blade has been divided into

triangular elements that might be used to find the temperature distribution or stress distribution in the blade. A variety of element shapes may be used, and different element shapes may be employed in the same solution region. Indeed, when analysing an elastic structure that has different types of components such as plates and beams, it is not only desirable but also necessary to use different elements in the same solution. Although the number and the type of elements in a given problem are matters of engineering judgment, the analyst can rely on the experience of others for guidelines.

2. **Select Interpolation Functions.** The next step is to assign nodes to each element and then choose the interpolation functions to represent the variation of the field variable over the element. The field variable may be a scalar, a vector, or a higher-order tensor. Often, polynomials are selected as interpolation functions for the field variable because they are easy to integrate and differentiate. The degree of the polynomial chosen depends on the number of nodes assigned to the element, the nature and number of unknowns at each node, and certain continuity requirements imposed at the nodes and along the element boundaries. The magnitude of the field variable as well as the magnitude of its derivatives may be the unknowns at the nodes.

3. **Find the Element Properties.** Once the finite element model has been established, the matrix equations expressing the properties of the individual elements can be determined.

4. **Assemble the Element Properties to Obtain the System Equations.** To find the properties of the overall system modelled by the network of elements we must "assemble" all the element properties. In other words, we combine the matrix equations expressing the behaviour of the elements and form the matrix equations expressing the behaviour of the entire system. The matrix equations for the system have the same form as the equations for an individual element but they contain many more terms because they include all nodes.

   The basis for the assembly procedure stems from the fact that at a node, where elements are interconnected, the value of the field variable is the same for each element sharing that node. A unique feature of the finite element method is that the system equations are generated by assembly of the individual element equations. In contrast, in the finite difference method the system equations are generated by

writing nodal equations.

5. **Impose the Boundary Conditions.** Before the system equations are ready for being solved, they must be modified to account for the boundary conditions of the problem. At this stage we impose known nodal values of the dependent variables or nodal loads.

6. **Solve the System Equations.** The assembly process gives a set of simultaneous equations that we solve to obtain the unknown nodal values of the problem. If the problem describes steady or equilibrium behaviour, then we must solve a set of linear or nonlinear algebraic equations. There are different standard solution techniques for solving these equations. If the problem is unsteady, the nodal unknowns are a function of time, and we must solve a set of linear or nonlinear ordinary differential equations.

7. **Make Additional Computations If Desired.** Many times we use the solution of the system equations to calculate other important parameters. For example, in a structural problem the nodal unknowns are displacement components. From these displacements we calculate element strains and stresses. Similarly, in a heat-conduction problem the nodal unknowns are temperatures, and from these we calculate element heat fluxes.

4.3. Mechanical variables and basic equations

An important advantage of the FEM is that its use is not restricted to certain structures. To achieve a uniform and clear presentation, an operator formulation is applied using matrix variables. The variables are divided into field and boundary variables.[3]

Basic mechanical equations:

$$\underline{\varepsilon} = \underline{D_k} \cdot \underline{u} \qquad \text{(Kinematic law)} \qquad (2)$$

$$\underline{\sigma} = \underline{E} \cdot \underline{\varepsilon} + \underline{D} \cdot \underline{\dot{\varepsilon}} \qquad \text{(Material law)} \qquad (3)$$

$$-(\underline{p} + \underline{f}) = \underline{D_G} \cdot \underline{\sigma} \qquad \text{(Dynamic equilibrium conditions)} \qquad (4)$$

[3] Subtracted from "Finite–Elemente–Methode der Statik und Dynamik"; Eller, C.

Features in these three basic equations:

$\underline{p}$ - Vector of external force variables

$\underline{u}$ - Vector of external displacement variables

$\underline{f}$ - Vector of d'Alembert inertial forces

$\underline{\sigma}$ - Vector of internal force variables

$\underline{\varepsilon}$ - Vector of internal displacement variables (Distortion, stretching, curvature)

Along the boundaries the following variables are defined:

$\underline{t}$ - Vector of boundary force variables

$\underline{r}$ - Vector of boundary displacements variables.

In addition, the static and geometric constraints must be satisfied at the boundaries of the mechanical system.

$$\underline{r} = \underline{R_r} \cdot \underline{u} \qquad \text{(Displacement boundary conditions)} \qquad (5)$$

$$\underline{t} = \underline{R_t} \cdot \underline{\sigma} \qquad \text{(Force variables of boundary conditions)} \qquad (6)$$

4.4. Equilibrium conditions of geometrically nonlinear structures

For the formulation of the equilibrium of complex structures energy statements instead of differential equations are used. Such an energy principle is the principle of virtual displacements.

The principle of virtual displacements is a global equilibrium formulation. It is based on the evidence that the sum of virtual work is zero.

$$\delta W = \delta W_i + \delta W_a = 0 \qquad \text{(The basic equation)} \qquad (7)$$

Thereafter, a deformed body is in balance if the internal and external virtual work due to a virtual displacement are identical:

$$\delta W_i = \delta W_a \qquad \text{(Equilibrium condition)} \qquad (8)$$

For the present thesis dealt with thin-walled shell structures, this principle is:

$$\int_A \underline{\sigma}^T \cdot \delta\underline{\varepsilon} \cdot dA = \int_A \underline{p}^T \cdot \delta\underline{u} \cdot dA + \int_{S_t} \underline{t}^T \cdot \delta\underline{r} \cdot dS_t \qquad (9)$$

As part of geometric non-linear theories, large structural deformations are taken into account. The basic kinematic equation in this case reads as

$$\varepsilon = \underline{D_k} \cdot \underline{u} = \left[\underline{D_{KL}} + \frac{1}{2} \cdot \underline{D_{KN}}\left(\underline{u}\right)\right] \cdot \underline{u} \qquad (10)$$

The kinematic operator $\underline{\mathrm{D}}_{\mathrm{k}}$ can be split into a deformation-independent linear partial operator $\underline{\mathrm{D}}_{\mathrm{KL}}$ and a deformation-dependent, nonlinear partial operator $\underline{\mathrm{D}}_{\mathrm{KN}}(\underline{\mathrm{u}})$.

The virtual strain $\delta\underline{\varepsilon}$ is obtained from Eq. (10) by variation.

$$\delta\underline{\varepsilon} = \frac{d\underline{\varepsilon}}{d\underline{u}} \cdot \delta\underline{u} = \left[\underline{D_{KL}} + \underline{D_{KN}}\left(\underline{u}\right)\right] \cdot \delta\underline{u} \qquad (11)$$

The material law for physically linear material behavior is:

$$\underline{\sigma} = \underline{E} \cdot \underline{\varepsilon} = \underline{E} \cdot \underline{D_K} \cdot \underline{u} \qquad (12)$$

The virtual boundary displacements $\delta\underline{r}$ are expressed with the boundary operator $\underline{R_r}$ by the field distribution displacements $\delta\underline{u}$:

$$\delta\underline{r} = \underline{R_r} \cdot \delta\underline{u} \qquad (13)$$

Setting equations (10) to (13) in the equilibrium requirement (9), yields:

$$\int_A \underline{u}^T \cdot \left[\underline{D_{KL}} + \frac{1}{2} \cdot \underline{D_{KN}}\left(\underline{u}\right)\right]^T \cdot \underline{E} \cdot \left[\underline{D_{KL}} + \underline{D_{KN}}\left(\underline{u}\right)\right] \cdot \delta\underline{u} \cdot dA =$$

$$= \int_A \underline{p}^T \cdot \delta\underline{u} \cdot dA + \int_{S_t} \underline{t}^T \cdot \underline{R_r} \cdot \delta\underline{u} \cdot dS_t \tag{14}$$

As a part of the finite element method, the deformations of the elements are approximated:

$$\underline{u} = \underline{\Omega} \cdot \underline{v} \tag{15}$$

and

$$\delta\underline{u} = \underline{\Omega} \cdot \delta\underline{v} \tag{16}$$

where $\underline{\Omega}$ denotes the matrix of shape function and $\underline{v}$ or $\delta\underline{v}$ represent the actual or virtual nodal displacements.

Inserting (15) and (16) into the equilibrium requirement (14), yields:

$$\delta\underline{v}^T \int_A \underline{\Omega}^T \cdot \left[\underline{D_{KL}} + \frac{1}{2} \cdot \underline{D_{KN}}\left(\underline{\Omega} \cdot \underline{v}\right)\right]^T \cdot \underline{E} \cdot \left[\underline{D_{KL}} + \underline{D_{KN}}\left(\underline{\Omega} \cdot \underline{vu}\right)\right] \cdot \underline{\Omega} \cdot \underline{v} \cdot dA =$$

$$= \delta\underline{v}^T \int_A \underline{\Omega}^T \cdot \underline{p} \cdot dA + \delta\underline{v}^T \int_{S_t} \underline{\Omega}^T \cdot \underline{R_r}^T \cdot \underline{t} \cdot dS_t \tag{17}$$

After the introduction of the linear and nonlinear strain displacement matrix:

$$\underline{H_L} = \underline{D_{KL}} \cdot \underline{\Omega} \tag{18}$$

$$\underline{H_N}(\underline{v}) = \underline{D_{KN}} \cdot (\underline{\Omega} \cdot \underline{v}) \cdot \underline{\Omega} \tag{19}$$

and simplified division by $\delta\underline{v}^T$, the equation (17) can be written as:

$$\int_A \left[\underline{H_L} + \underline{H_N}(\underline{v})\right]^T \cdot \underline{E} \cdot \left[\underline{H_L} + \frac{1}{2} \cdot \underline{H_N}(\underline{v})\right]^T \cdot dA \cdot \underline{v} =$$

$$= \int_A \underline{\Omega}^T \cdot \underline{p} \cdot dA + \int_{S_t} \underline{\Omega}^T \cdot \underline{R_r}^T \cdot \underline{t} \cdot dS_t \tag{20}$$

This non-linear relationship for the element equilibrium cannot be solved and may require numerical solution methods. For this, the force and deformation variables are incremented, i.e. they are split into the fundamental state assumed to be known (-) and the increments (+).

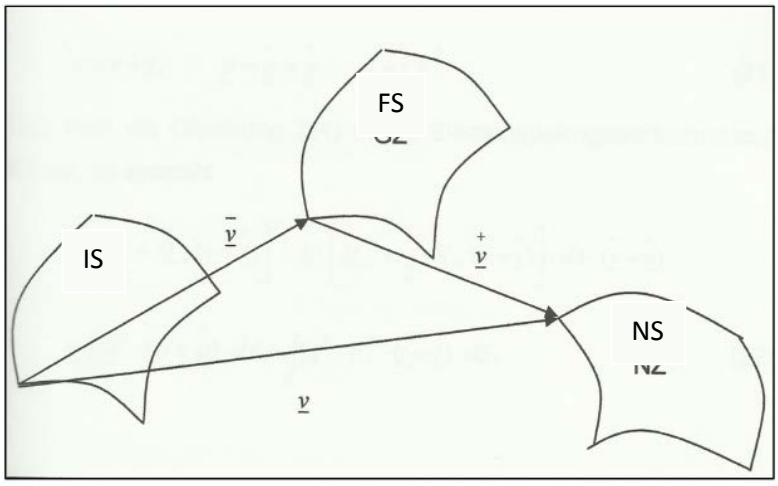

Figure 20: Fundamental state and increase parameters

IS – Initial state

FS - Fundamental increment

NS - Neighboring increment

In the figure below the mentioned states are demonstrated visually for both axial and radial pressure:

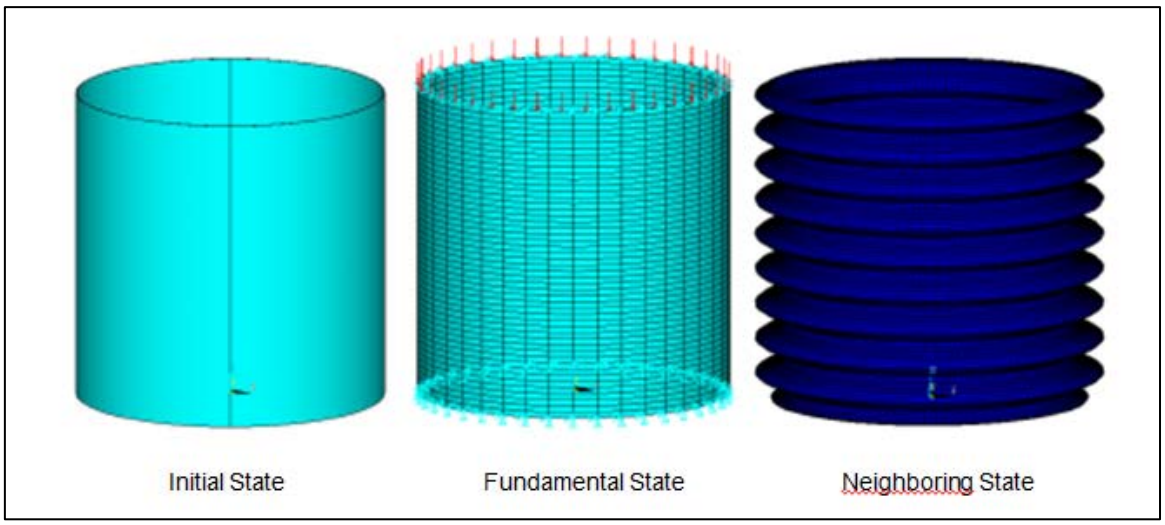

Figure 21: Visual demonstration of the states under axial pressure.

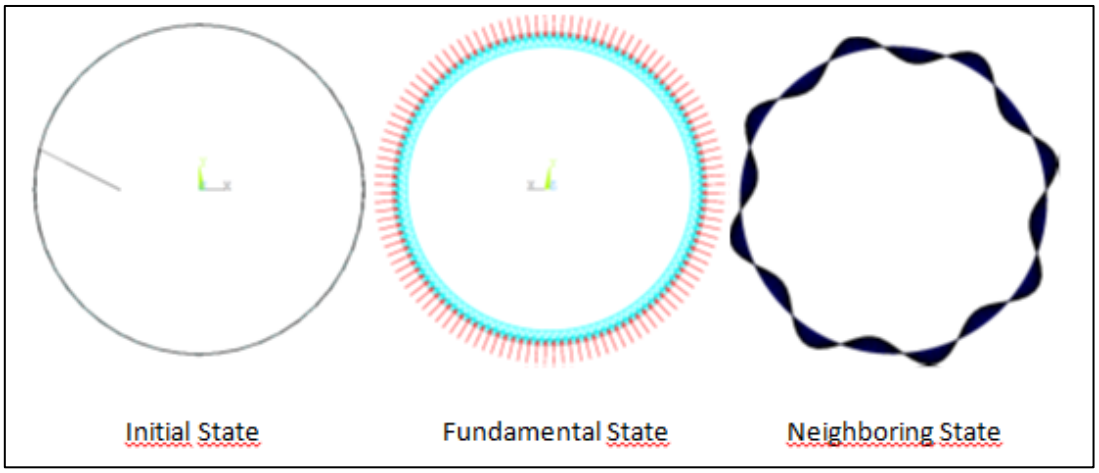

Figure 22: Visual demonstration of the states under radial pressure.

It is therefore:

$$\underline{v} = \underline{v}^- + \underline{v}^+; \qquad \underline{p} = \underline{p}^- + \underline{p}^+; \qquad \underline{t} = \underline{t}^- + \underline{t}^+; \tag{21}$$

Introducing the equation (21) into the equilibrium equation (20), yields:

$$\int_A \left[\underline{H_L} + \underline{H_N}(\underline{v}^- + \underline{v}^+)\right]^T \cdot \underline{E} \cdot \left[\underline{H_L} + \frac{1}{2} \cdot \underline{H_N}(\underline{v}^- + \underline{v}^+)\right]^T \cdot dA \cdot (\underline{v}^- + \underline{v}^+) =$$

$$= \int_A \underline{\Omega}^T \cdot (\underline{p}^- + \underline{p}^+) \cdot dA + \int_{S_t} \underline{\Omega}^T \cdot \underline{R_r}^T \cdot (\underline{t}^- + \underline{t}^+) \cdot dS_t \tag{22}$$

After multiplying out and sorting results, the following element matrices and vectors arise:

- Elastic stiffness matrix:

$$\underline{k_e} \cdot \underline{v}^+ = \int_A \underline{H_L}^T \cdot \underline{E} \cdot \underline{H_L} \cdot dA \cdot \underline{v}^+$$

- Linear initial stress matrix:

$$\underline{k_{\sigma L}} \cdot \underline{v}^+ = \int_A \underline{H_N}^T(\underline{v}^+) \cdot \underline{E} \cdot \underline{H_L} \cdot \underline{v}^- \cdot dA$$

- Nonlinear initial stress matrix:

$$\underline{k}_{\sigma N} \cdot \underline{v}^{+} = \int_A \frac{1}{2} \cdot \underline{H}_N{}^T(\underline{v}^{+}) \cdot \underline{E} \cdot \underline{H}_N \cdot (\underline{v}^{-}) \cdot (\underline{v}^{-}) dA \tag{23}$$

- Linear initial deformation matrix:

$$\underline{k}_{uL} \cdot \underline{v}^{+} = \int_A (\underline{H}_L{}^T \cdot \underline{E} \cdot \underline{H}_N \cdot (\underline{v}^{-}) + \underline{H}_N{}^T(\underline{v}^{-}) \cdot \underline{E} \cdot \underline{H}_L) \cdot dA \cdot \underline{v}^{+}$$

- Nonlinear initial deformation matrix:

$$\underline{k}_{uN} \cdot \underline{v}^{+} = \int_A \left(\underline{H}_N{}^T \cdot (\underline{v}^{-}) \cdot \underline{E} \cdot \underline{H}_N \cdot (\underline{v}^{-})\right) \cdot dA \cdot \underline{v}^{+}$$

- Vector of internal forces in the fundamental state:

$$\underline{g} \cdot \underline{v}^{+} = \int_A \left[\underline{H}_L + \underline{H}_N \cdot (\underline{v}^{-})\right]^T \cdot \underline{E} \cdot \left[\underline{H}_L + \frac{1}{2} \cdot \underline{H}_N(\underline{v}^{-})\right] \cdot \underline{v}^{-} \cdot dA$$

- Element load vector in the fundamental state:

$$\underline{p}^{-} = \int_A \underline{\Omega}^T \cdot \underline{p}^{-} \cdot dA + \int_{S_t} \underline{\Omega}^T \cdot \underline{R}_r{}^T \cdot \underline{t}^{-} \cdot dS_t$$

- Incremental load vector

$$\underline{p}^{+} = \int_A \underline{\Omega}^T \cdot \underline{p}^{+} \cdot dA + \int_{S_t} \underline{\Omega}^T \cdot \underline{R}_r{}^T \cdot \underline{t}^{+} \cdot dS_t$$

Adding up all the element-related matrices, we obtain the tangential element stiffness matrix

$$\underline{k}_T = \underline{k}_e + \underline{k}_{\sigma L} + \underline{k}_{\sigma N} + \underline{k}_{uL} + \underline{k}_{uN} \tag{24}$$

With the introduced matrices and vectors, the element equilibrium relationship can be converted into the following matrix representation:

$$\underline{k}_T \cdot \underline{v}^{+} = \left(\underline{k}_e + \underline{k}_{\sigma L} + \underline{k}_{\sigma N} + \underline{k}_{uL} + \underline{k}_{uN}\right) \cdot \underline{v}^{+} = \underline{p} - \underline{g} \cdot (\underline{v}^{-}) \tag{25}$$

After the assembly of the finite elements, the system tangential stiffness relationship reads as:

$$\underline{K_T} \cdot \underline{V}^+ = \left(\underline{K_e} + \underline{K_{\sigma L}} + \underline{K_{\sigma N}} + \underline{K_{uL}} + \underline{K_{uN}}\right) \cdot \underline{V}^+ = \underline{P} - \underline{G} \cdot (\underline{V}^-) \tag{26}$$

For the application of line-search algorithms, the load is incremented, i.e. divided into small load steps. Within this last step, equation (26) is solved iteratively until the right side is zero.

An algorithm that has proved is the Newton - Raphson – scheme, rebuilding the tangential stiffness matrix with each iteration step. (See figure 20)

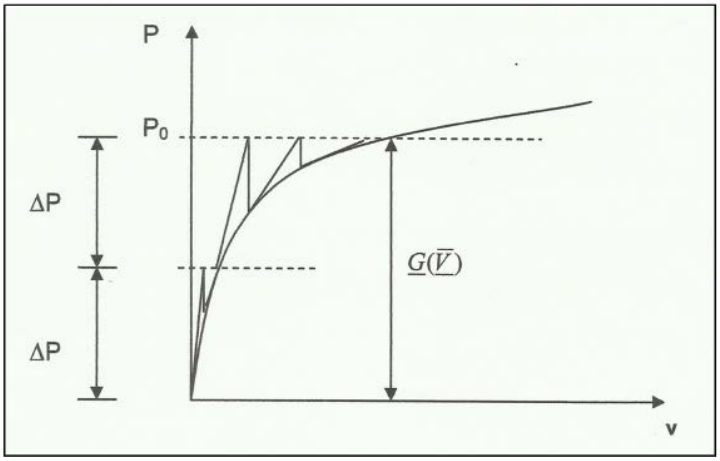

Figure 23: Newton-Raphson algorithm

In geometrically linear investigations the arising deformations $\underline{V}$ are by definition very small. The fundamental state can be connected to the output state ($\overline{\underline{V}} = 0$). The deformation vector $\underline{V}^+ = \underline{V}$ then describes the sought displacement field. The only system matrix remaining independent of the fundamental state deformations is the elastic stiffness matrix, so that from equation (26) the following linear system of equations results:

$$\underline{K_e} \cdot \underline{V} = \underline{P} \tag{27}$$

The total stiffness matrix $\underline{K_e}$ is symmetric and positive definite, so that efficient solution algorithms such as the Cholesky - procedures can be used.

4.5. Stability Analysis

In the implementation of stability testing is most sought after, whether next to a given equilibrium state (fundamental state $\underline{\overline{V}}$) an adjacent equilibrium position (adjacent state $\underline{V}^+$) without changing the external load is possible. If the deformation vector $\underline{\overline{V}}$ describes a balanced state of equilibrium, then the right side of the equation (26) is zero, because the external loads P and the internal stresses $\underline{G}(\underline{\overline{V}})$ are in equilibrium.

The desired equilibrium position in the adjacent state (neighboring state $\underline{V}^+$) shall occur at unmodified load. The equilibrium condition according to equation (26) reads as:

$$\underline{K_T} \cdot \underline{V}^+ = \underline{0} \tag{28}$$

with the vector $\underline{V}^+ \neq \underline{0}$.

Equation (28) describes a homogeneous system of equations. For non-trivial solution $\underline{V}^+$ the determinant of the coefficient matrix $\underline{K_T}$ has to be zero. Adjacent equilibrium positions are therefore only possible if

$$\det \underline{K_T} = 0 \tag{29}$$

This criterion can be examined by the incremental-iterative path-following after each step load balanced by an accompanying eigenvalue calculation. If one eigenvalue of $\underline{K_T}$ is equal to zero, so will be $\det \underline{K_T} = 0$, there is an instability point.

As part of this thesis circular cylindrical shells under radial load will be investigated. Therefore the fundamental state occurs in only radial deformation, leading to a so called linear prebuckling state. The initial deformation matrices $\underline{K_{uL}}$ and $\underline{K_{uN}}$ are zero in this case. Assuming further that the fundamental state deformations arising are small, so quadratic terms $\underline{\overline{V}}$ are ignored. This means that the nonlinear initial stress matrix $\underline{K_{\sigma N}}$ is negligibly small. Equation (28) is simplified thus:

$$(\underline{K_e} + \underline{K_{\sigma L}}) \cdot \underline{V}^+ = \underline{0} \tag{30}$$

In the computer-based implementation of stability analysis, the structure with a reference load ${}^0\underline{P}$ (e.g. $q_0 = 1\,N/mm^2$) is loaded and determines the increase in load factor λ_{Kr} in which an

instability occurs. Considering this approach in the above equation (30), one gets the initial value problem of the so-called “classical stability”:

$$(\underline{K_e} + \lambda_{Kr} \cdot \underline{K_{\sigma L}}({}^{0}\underline{P})) \cdot \underline{V}^{+} = \underline{0} \tag{31}$$

From the solution of this eigenvalue problem, the critical load factors λ and the corresponding buckling modes $\underline{V}^{+}$ are obtained. For the solution of the eigenvalue problem (see equation 31) the Lanczos algorithm was used in the present study.

5. FINITE ELEMENT MODELLING WITH ANSYS

5.1. Introduction

ANSYS is a general purpose finite element modeling package for solving different mechanical problems numerically, such as static/dynamic structural analysis, heat transfer and fluid problems, as well as acoustic and electro-magnetic problems.

ANSYS is divided into three steps when analyzing and solving a problem with the finite element method:

1. Preprocessing: It is basically defining the problem; the major steps in preprocessing are given below:

    - Define key-points, nodes, lines, areas, volumes.
    - Define element type and geometric properties.
    - Meshing.

2. Solution: the following steps should be specify before solving the problem:

    - Type of analysis: static, modal, buckling,…
    - Loads: point load or pressure, direction of the load,…
    - Constraints.

3. Post-processing: Viewing of the results, such as:

    - Lists of nodal displacements and displacement plots.
    - Element forces and moments.
    - Stress contour diagrams.

5.2. Buckling with ANSYS

Two techniques are available in ANSYS for predicting the buckling load and buckling mode of a structure:

- Nonlinear buckling analysis
- Eigenvalue buckling analysis.

5.2.1. Eigenvalue buckling analysis

Eigenvalue buckling analysis predicts the theoretical buckling strength of an ideal elastic structure. This analysis is used to predict the bifurcation point using a linearized model of elastic structure. It computes the structural eigenvalues for the given system loading and constraints. This is known as classical Euler buckling analysis.

However, in real-life, structural imperfections and nonlinearities prevent most real-world structures from reaching their eigenvalue predicted buckling strength. That means that this method over-predicts the expected buckling loads. That is the reason why it is not recommended for accurate, real-world buckling prediction analysis.

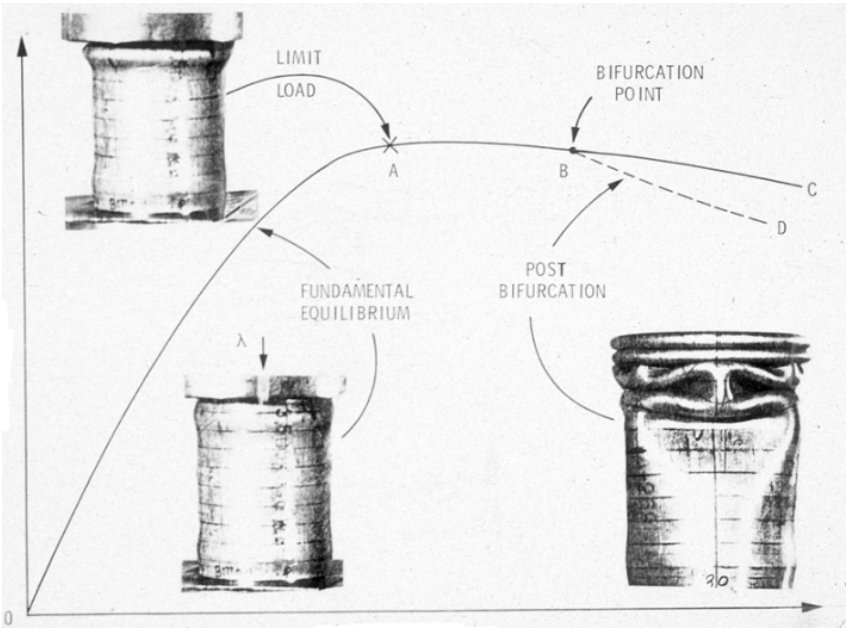

Figure 24: End shortening vs Axial load

The basic form of the eigenvalue buckling analysis is given by:

$$[\underline{K_e}]\{\emptyset_i\} = \boldsymbol{\lambda_i}[\underline{K_{\sigma L}}]\{\emptyset_i\}$$

where

$[\underline{K_e}]$ = Elastic stiffness matrix

$\{\emptyset_i\}$ = Eigen vector

$\boldsymbol{\lambda_i}$= Eigen value for buckling mode

$[\underline{K_{\sigma L}}]$ = Initial stress matrix. This matrix includes the effects of membrane loads on the stiffness of the structure. It is also assembled based on the results of a previous linear static analysis.

The eigenvalue solution uses an iterative algorithm that obtains at first the eigenvalues and secondly the displacements that define the corresponding mode shape.

The eigenvalue represents the ratio between the applied load and the buckling load. This can be expressed as follows:

$$\boldsymbol{\lambda_i = \frac{Buckling\ Load}{Applied\ Load}}$$

That's why it is often said that the eigenvalue is like a safety factor for the structure against buckling. On one hand, an eigenvalue less than 1.0 indicates that a structure has buckled under the applied loads. On the other hand, an eigenvalue greater than 1.0 indicates that the structure will not buckle.

Another important point to note about this formulation is that only the membrane component of the loads in the structure is used to determine the buckling load. This means that the effect of prebuckling rotations due to moments is ignored.

5.2.2. Nonlinear buckling analysis

It is more accurate than eigenvalue analysis because it employs non-linear, large-deflection, static analysis to predict buckling loads. Its mode of operation is very simple: the applied load is gradually increased until a load level is found whereby the structure becomes unstable. Normally each of these load increments will converge in a small number of iterations.

It is also common that suddenly a very small increase in the load cause very large deflections.

The nonlinear solver is ideally suited for modeling structures that do not collapse while buckling. In the nonlinear analysis the stiffness matrix is updated periodically (for every iteration of every load increment) based on the current deformed shape of the structure. This is important from a buckling point of view since the effect of the pre - and post-buckling deformations are included in the analysis. When we talk about 'pre-buckling deformations' we are generally referring to those deflections caused by the moments in the structure prior to buckling. 'Post buckling deformations' refers to those deflections that result from some initial buckling failure of the structure.

It also permits the modeling of geometric imperfections, load perturbations and gaps. Another important point that should be made about the nonlinear buckling analysis is that material nonlinearities (yielding) can be considered in addition to the geometric effects.

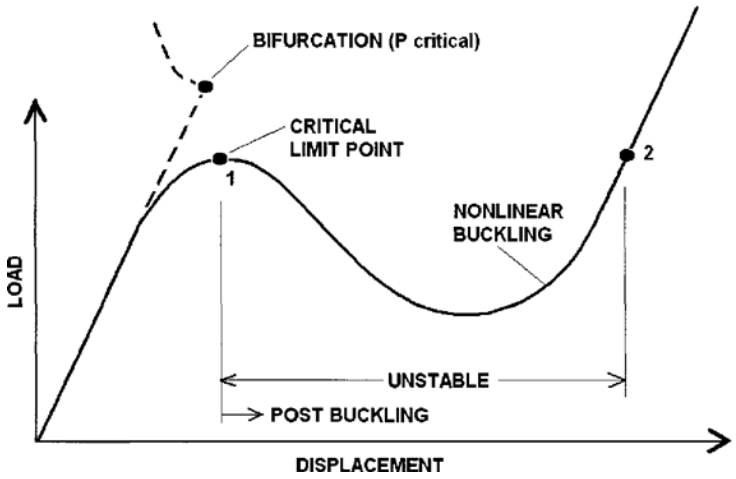

Figure 25: Buckling

5.3. ANSYS Elements

To carry out the simulations of our project, two different elements from ANSYS library will be used:

- SOLID 45
- SHELL 63

5.3.1. SOLID 45

This element is used for three-dimensional modeling of solid structures. The element is defined by eight nodes, having three degrees of freedom at each node: translations in the nodal x, y, and z directions.

The element has plasticity, creep, swelling, stress stiffening, large deflection, and large strain capabilities.

Pressures may be input as surface loads on the element faces and positive pressures act into the element. Temperatures and fluencies may be input as element body loads at the nodes.

The geometry, node locations, and the coordinate system for this element are shown in the following figure:

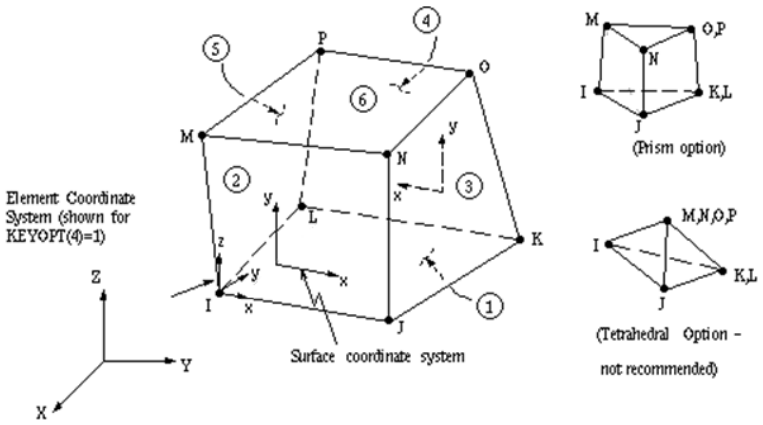

Figure 26: SOLID 45

5.3.2. SHELL 63

It has both bending and membrane capabilities. Both in-plane and normal loads are permitted. The element has six degrees of freedom at each node: translations in the nodal x, y, and z directions and rotations about the nodal x, y, and z axes.

Stress stiffening and large deflection capabilities are included. A consistent tangent stiffness matrix option is available for use in large deflection analyses.

The geometry, node locations, and the coordinate system for this element are shown in the following figure:

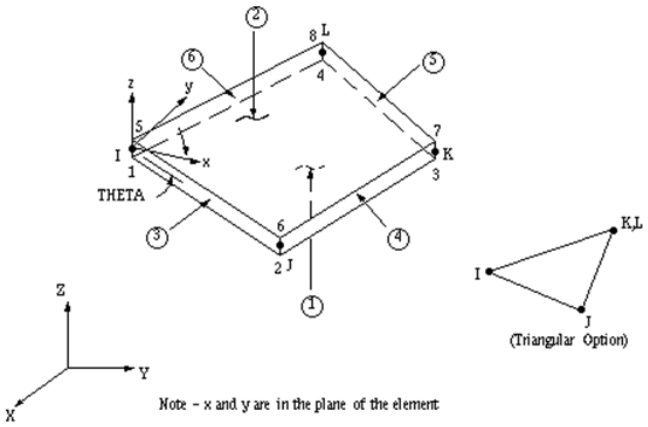

Figure 27: SHELL63

The element is defined by four nodes, four thicknesses, an elastic foundation stiffness, and the orthotropic material properties and the thickness is assumed to vary smoothly over the area of the element.

Pressures may be input as surface loads on the element faces and positive pressures act into the element. Edge pressures are input as force per unit length. The lateral pressure loading may be an equivalent element load applied at the nodes or distributed over the face of the element.

The equivalent element load produces more accurate stress results with flat elements representing a curved surface or elements supported on an elastic foundation since certain fictitious bending stresses are eliminated.

6. LINEAR STABILITY ANALYSIS OF CIRCULAR CYLINDRICAL SHELLS UNDER AXIAL LOAD

6.1. Analysis of perfect cylindrical shells under axial load

6.1.1. Introduction

In this part, the stability calculations using the finite element program ANSYS will be carried out. Fig. 28 represents the meshed cylindrical shell with the boundary conditions applied.

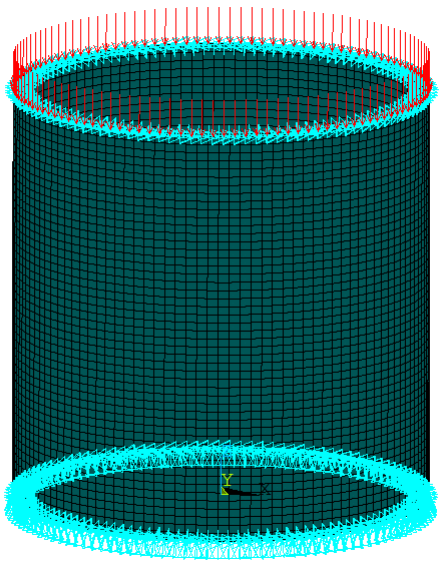

Figure 28: Model studied with ANSYS. Boundary conditions.

The structure is supported at the bottom, restricting displacements in the three directions, and at the top of the shell only the axial direction is free. The load is applied axially. The initial phase of the investigation is carried out on a perfect cylindrical shell subjected to uniformly distributed load. Then the analytical solution is compared with the results calculated with

ANSYS. In the course of this chapter, different configurations of axial loads will be studied:

- Buckling analysis of cylindrical shell under uniform axial load.
- Buckling analysis of cylindrical shell under partial axial load.
- Buckling analysis of cylindrical shell under triangularly distributed axial load.

The referent material will be steel.

6.1.1.1. Specifications

In this section, the configuration of the regular cylindrical shell is described. The task is formulated in a framework that makes room for assumptions and simplifications. Furthermore, assumptions and predefined values are briefly described.

The geometric and material input parameters are listed in the following list:

- Radius: R=5000 mm
- Height: L=10000 mm
- Shell thickness: t=20 mm
- Young's modulus: E=2.1 x 10^5 N/mm^2
- Poisson's Ratio: $\nu = 0.3$
- Axial Load: P=1 MPa

A cylindrical coordinate system is introduced. The ANSYS internal name of the coordinate directions is as follows:

• X: Radial direction

• Y: Circumferential direction

• Z: Axial direction

All ANSYS plots of sections, sizes and displacement refer to this coordinate system. At the bottom, at Z = 0, the displacements in X, Y, Z directions are restricted. At the top, Z = 10000, the displacements in X and Y directions are also restricted. The Z direction is free.

6.1.1.2. Discretization and mesh. Validation of the model

The classical buckling stress of axially compressed cylinder is shown in the equation.

The classical calculation is independent of the buckling form. However, it shall apply only to purely axially loaded cylinders with classic bearing (see Figure 24).

The classical calculation, under an axial compression of P = 1N/mm, gives a result of:

$$\boldsymbol{\sigma_{cr}} = \frac{E \cdot t}{R\sqrt{3(1-\nu^2)}} = \frac{2{,}1 \cdot 10^5 \cdot 20}{5000\sqrt{3(1-0{,}3^2)}} = \mathbf{508{,}391}\,\frac{\boldsymbol{N}}{\boldsymbol{mm^2}}$$

To make a comparative calculation, the classical bearing is adopted and the Solid-45 element is used.

Total number of elements	Circumferential direction	Axial direction	Radial direction	Critical load ANSYS (MPa)	Error (%)	Analytical solution load (MPa)	Computing time (s)
12000	120	50	2	514,38	0,63	511,164	10,79

Chart 1: Analysis with Solid-45

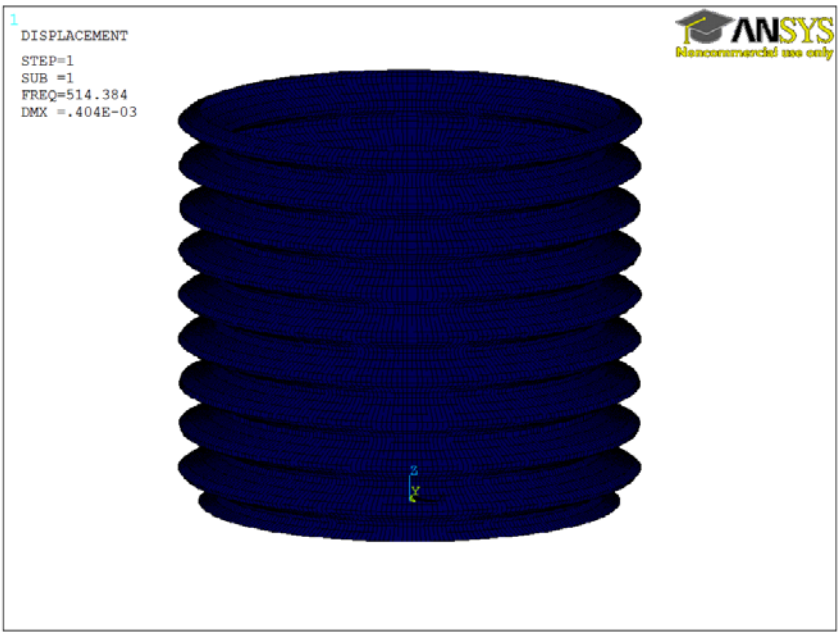

Figure 29: Model studied with Solid-45 after buckling analysis

It can be seen that the analytical solution and the one given by ANSYS differ in just 0,63 %.

If another comparative calculation with element Shell-63 is made, it is necessary to modify the classical buckling stress, because the element Shell-63 is defined by four nodes. It is a flat element so the thickness must be taken on account:

$$\boldsymbol{\sigma_{cr}} = \frac{E\,t^2}{R\sqrt{3(1-\nu^2)}} = \frac{2{,}1\cdot 10^5\cdot 20^2}{5000\sqrt{3(1-0{,}3^2)}} = \boldsymbol{10167{,}82\,\frac{N}{mm}}$$

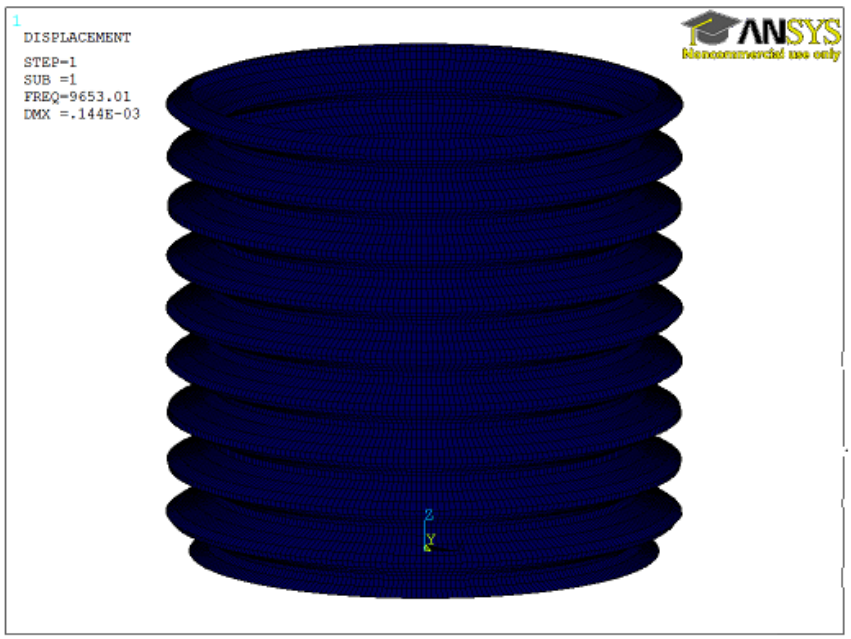

Figure 30: Model studied with Shell-63 after buckling analysis

The required mesh fineness is determined by preliminary investigations when setting up the model. Often, the calculated values with the program are not the reality. This error can be reduced, interpreting the calculations with a very fine mesh. The statement is complicated and requires very high computing time. But only one obtained result attain to match the reality.

Now, the circular cylindrical shell with different mesh densities is investigated. The decision of what mesh distribution for the analysis is most suitable will be taken based on these calculations.

The following chart shows the results as a function of different numbers of elements in the circumferential and the axial direction for Shell-63.

Number of elements	Circumferential direction	Axial direction	Radial direction	Critical load ANSYS (MPa)	Error (%)	Analytical solution load (MPa)	Computing time (s)
10000	200	50	1	9223,78	10,23	10167,82	15,55
14400	240	60	1	9484,19	7,20	10167,82	26,93
19600	280	70	1	9653,01	5,33	10167,82	37,64
25600	320	80	1	9726,05	4,54	10167,82	54,27

Chart 2: Analysis with Shell-63

The eigenvalues calculated with ANSYS almost agree with the value of the classical calculation.

On one hand, it is possible to see that the error is bigger when the mesh is rougher (it has less elements). On the other hand, the computational time and memory capacity of the computer needed by the fine mesh is much bigger when calculating a fine mesh than the rough mesh.

In the diagrams below, the number of elements of the mesh and the error committed by ANSYS are represented as a function of the time needed to calculate the critical load.

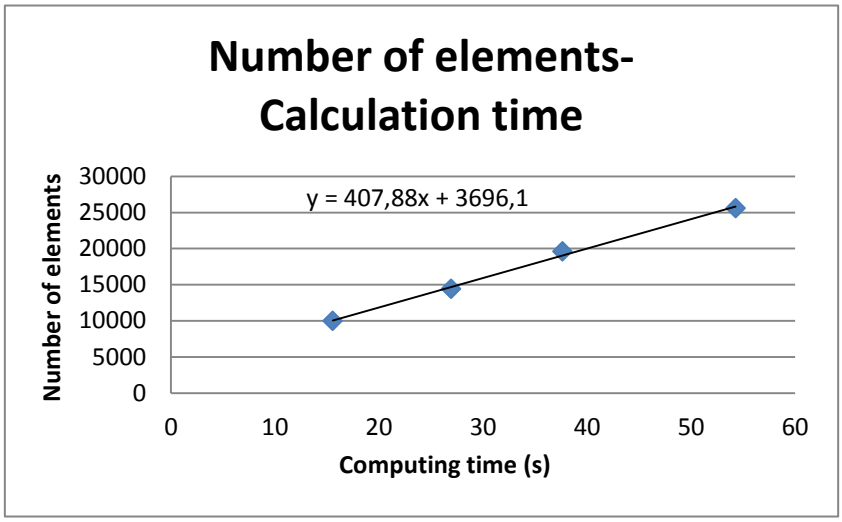

Diagram 1: Number of elements of the model with Shell-63 vs. computing time

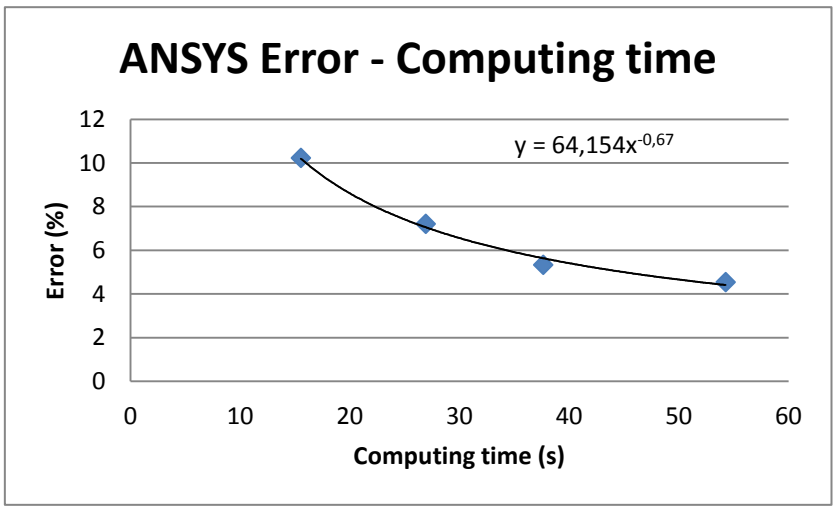

Diagram 2: Error committed by ANSYS vs. computing time

Diagram 1 can thus be used to predict the computing time that might be needed to calculate the critical load with a specific mesh fineness, always taking on account that with the version ANSYS 14.0, the number of elements cannot exceed 32000.

There is a clearly defined pattern to the Diagram 2, and this can be taken to mean that to obtain a precise solution with ANSYS, a long calculating time is required.

To sum up, for a good analysis, the accurate combination between fineness and time has to be found.

According to the results obtained and the relation error between analytical solution and ANSYS solution-computing time, in the following models with Shell-63, a distribution mesh with a total number of 19600 elements will be used; models designed with Solid-45 will have a total number of 12000 elements.

6.1.2. Buckling analysis of a perfect cylindrical shell under partial axial load, using Shell-63 and Solid-45.

In this chapter, the behavior of a perfect cylindrical shell subjected to non-uniform axial load will be studied. This means, that the difference in critical load depending on the angle of application of the load will be analyzed. The test will be carried out with a load of 1 MPa.

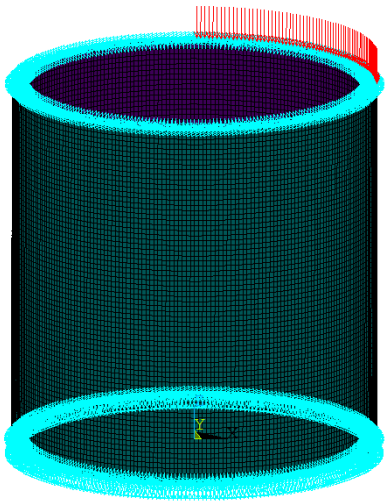

Figure 31: Model under 90^0 axial load

Firstly, the model designed with Shell-63 will be analyzed. The next table shows the results of the critical buckling load obtained for each angle, as well as the maximum displacement for each value.

α (°)	Critical Load (MPa)
30	10028,2
60	9744,19
90	9220,23
120	8523,93
150	8153,32
180	7990,31
210	7948,19
240	7995,25
270	8162,29
300	8503,19
330	9211,63
360	9653,01

Chart 3: Critical load as a function of the load angle with Shell-63

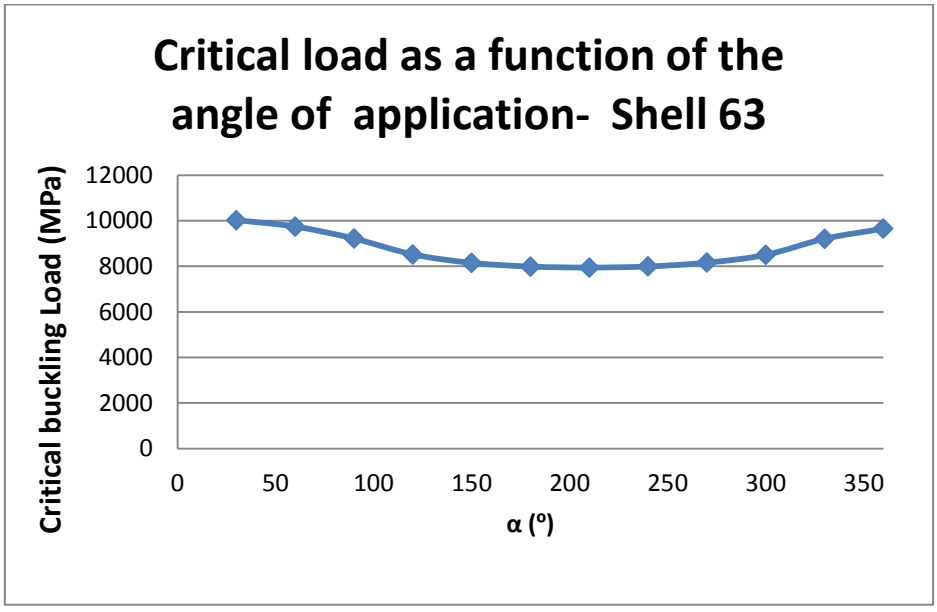

Diagram 3: Variation of the critical load depending on the angle of application with Shell-63

It can be observed that the critical buckling load depends on the angle of application of the load, although not in a downward trend, as it could be expected a priori.

The next images show the buckling deformation pattern for the following values of the angle of application: 90°, 180°, 270° and 360°.

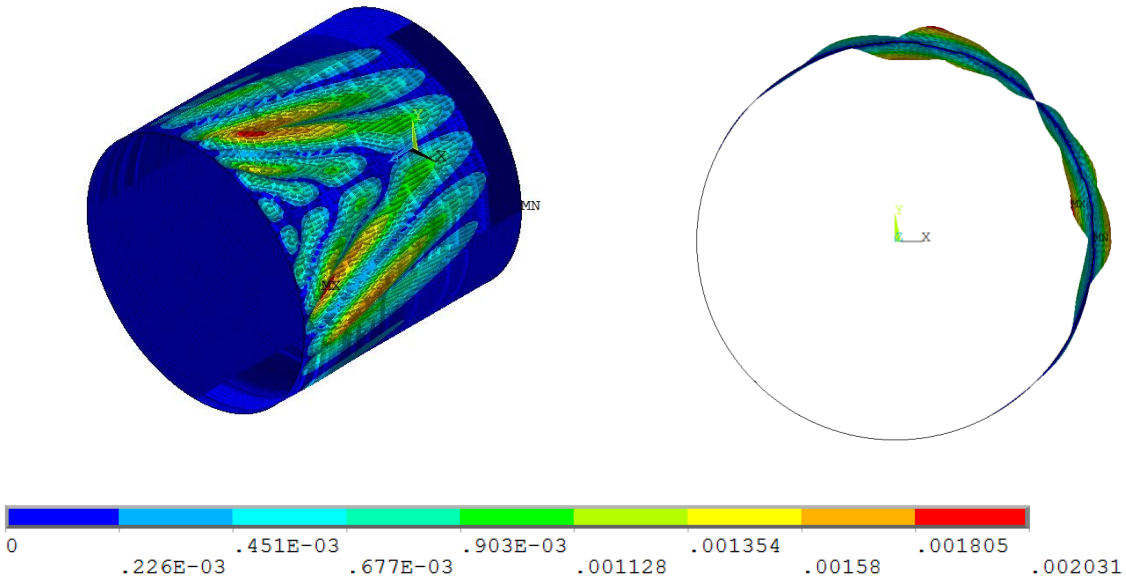

Figure 32: Deformed cylinder when is subjected to 90 ^{o} axial load

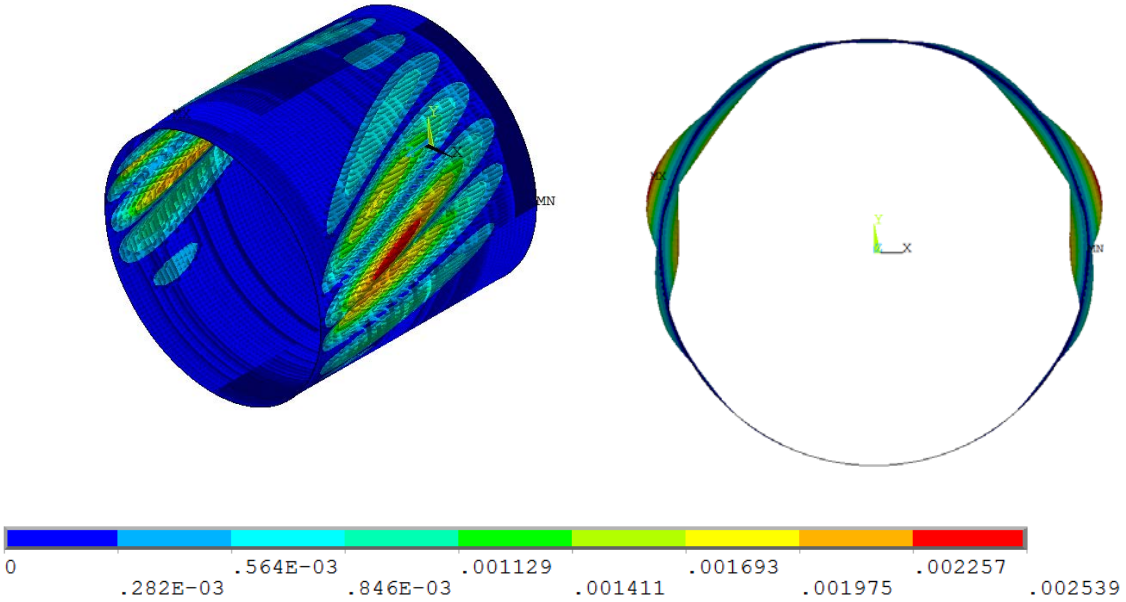

Figure 33: Deformed cylinder when is subjected to 180 ^{o} axial load

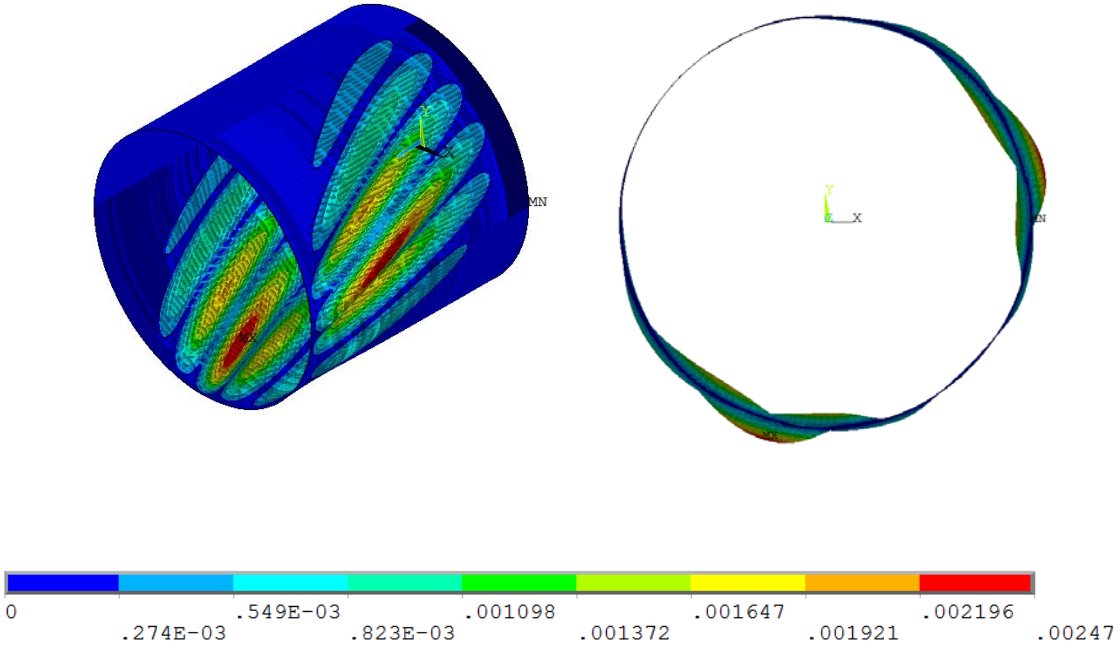

Figure 34: Deformed cylinder when is subjected to 270 ^{o} axial load

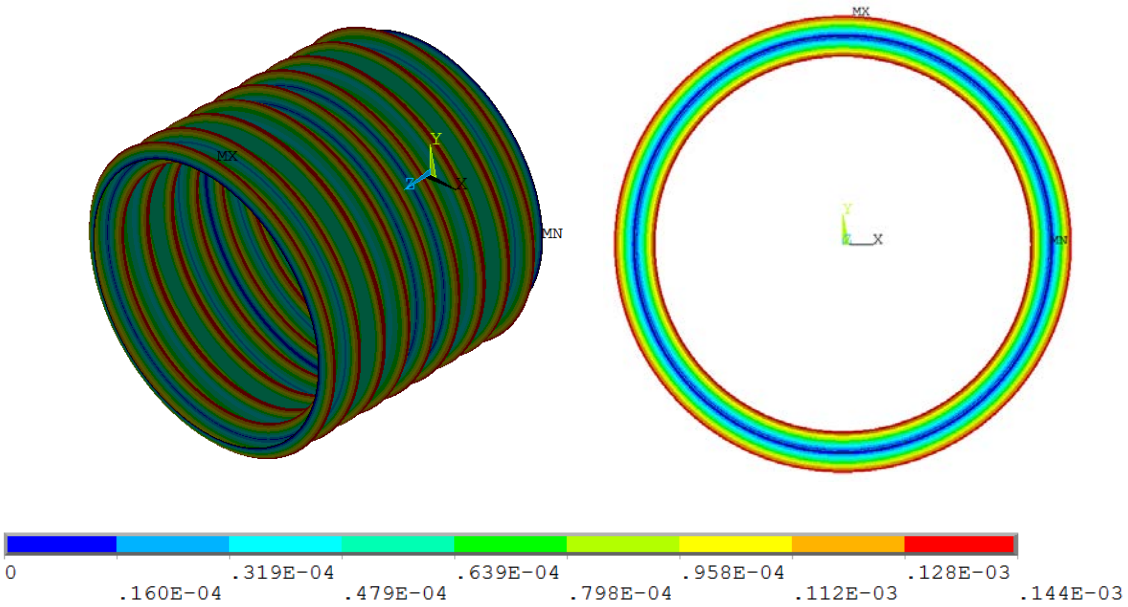

Figure 35: Deformed cylinder when is subjected to 360 ^{o} axial load

To ensure the results obtained with Shell-63, the same experiment is carried out with the element Solid-45.

α (°)	Critical Load (MPa)
30	595,8069
60	550,2982
90	538,43765
120	496,78005
150	474,3563
180	465,06965
210	462,52285
240	465,5503
270	475,6823
300	496,8563
330	516,21985
360	514,38435

Chart 4: Critical load as a function of the load angle with Shell-63

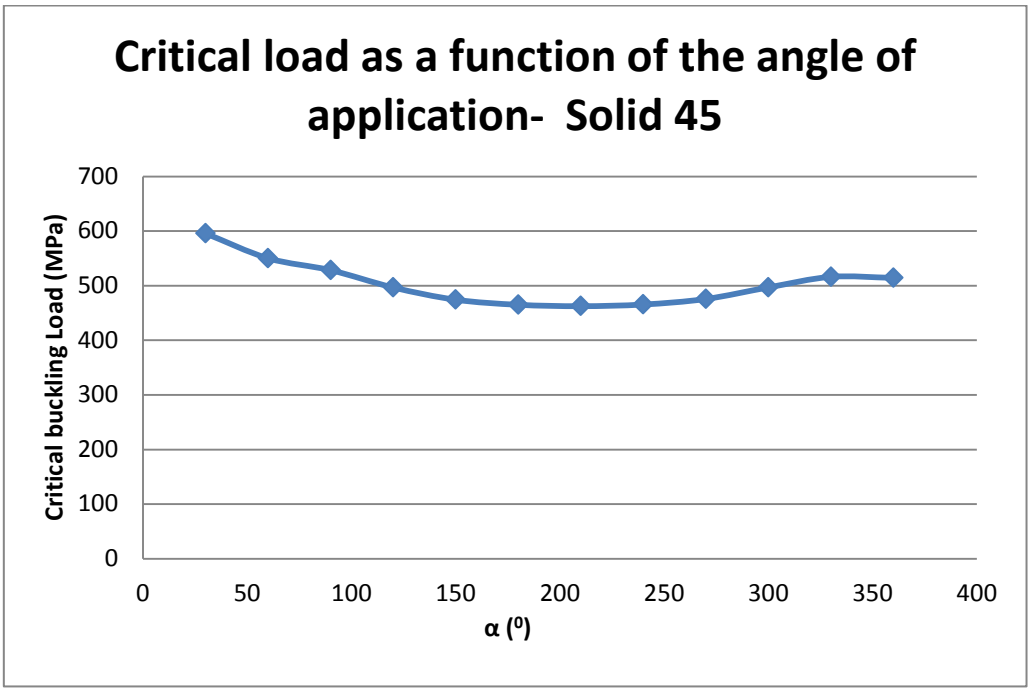

Diagram 5: Critical load as a function of the angle of application with Solid- 45

The experiment with Solid-45 confirms that, for both models, the minimum load needed by a steel cylinder to buckle is provided when the angle of application of load lays between 150º and 210 º. The maximum values are given when the angle is minimal, and the load applied tends to a punctual load.

6.1.3. Buckling analysis of a perfect cylindrical shell under triangularly distributed axial load, using Shell-63 and Solid-45.

In this section, the behavior of the same model will be investigated under varying load. This varying load consists of two triangularly distributed loads: One with encreasing slope, from 0 to 180°, and the second one with decreasing slope, from 180 to 360°. In addition to this, different values for that slope will be studied.

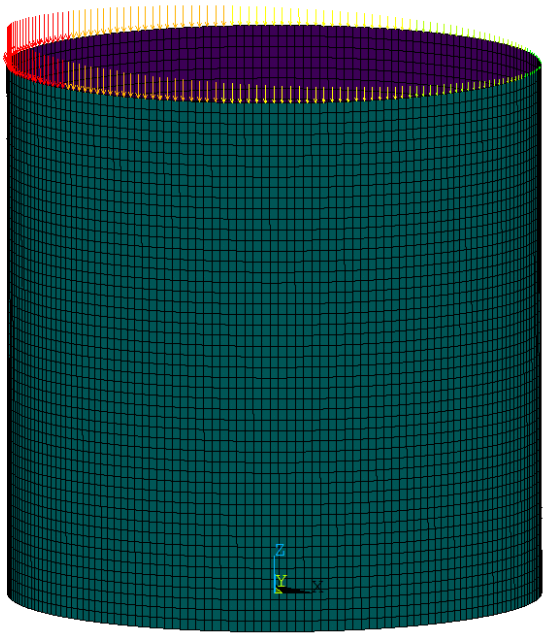

Figure 36: Model under triangularly distributed AXIAL LOAD

Slope (MPa/°)	Critical load (MPa)
0,02	2232,4
0,04	1265,3
0,06	882,755
0,08	677,81
0,1	550,093
0,15	373,939
0,2	283,238
0,3	190,717
0,4	143,758
0,6	96,3237
0,8	72,426
1	58,0291

Chart 5: Critical load as a function of the triangularly distributed load's slope

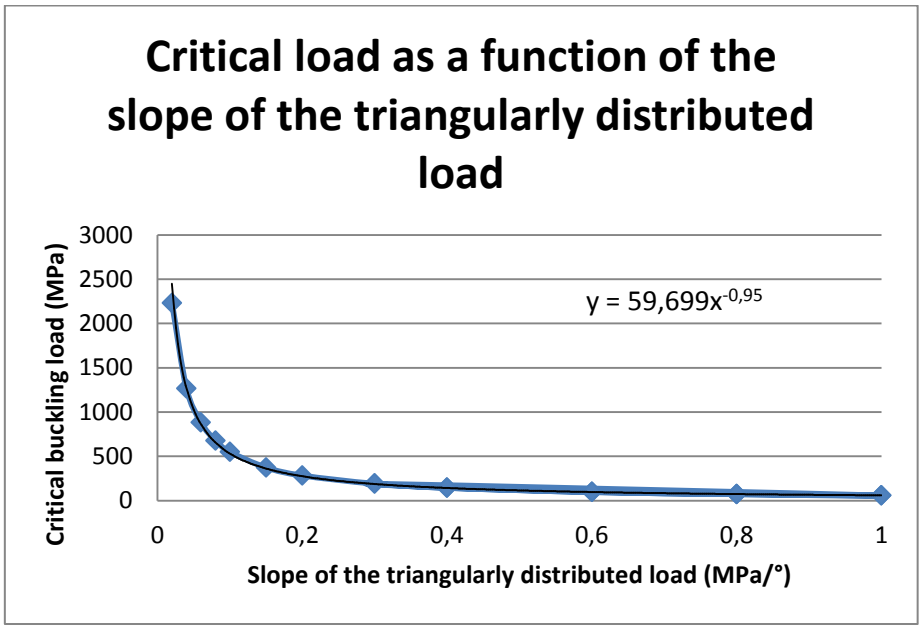

Diagram 6: Critical load as a function of the slope of the triangularly distributed load

As the diagram evidences, the critical buckling load decreases when increasing the slope of the triangularly distributed load. However, these downward trend differs from a straight line, and can be approximated by the power function $y = 59{,}699x^{-0{,}95}$.

This function can be used to predict the critical buckling load for any axial triangularly distributed load applied over the cylinder under study.

6.2 Analysis of cylindrical shells with variable section under axial load

6.2.1. Introduction

In this section, a cylindrical shell with a gradual variation of thickness along the shell will be investigated under the action of several distributions of axial load. To reach this aim, the element Solid-45 will be used, as a three dimensional element is needed to provide the gradual change of thickness. The dimensions of the model are specified in the next figure and material properties remain the same as for the perfect cylindrical shell, as well as the restrictions. The tests of these sections will be the same as for the constant wall cylinder, so that they can be compared after being studied.

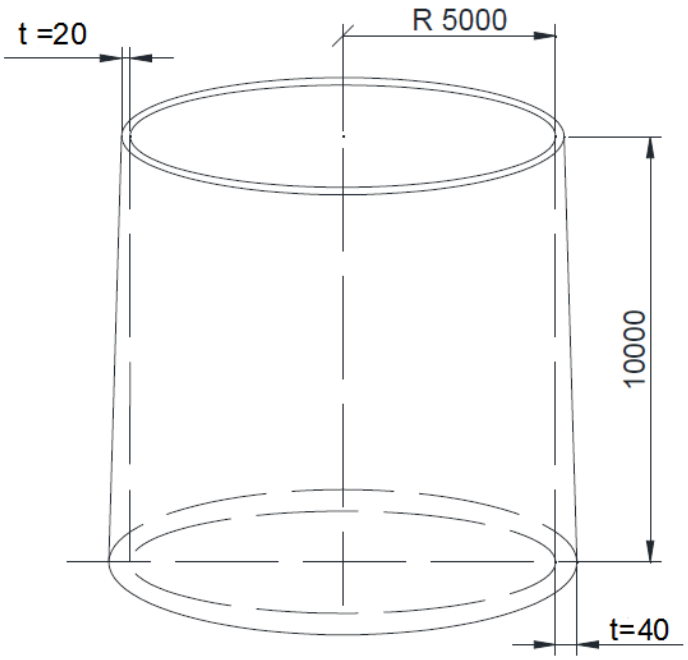

Figure 37: Measurements of the cylinder with variable thickness wall

6.2.2 Buckling analysis of a cylindrical shell with variable section under partial axial load.

In this moment, the model described above will be studied under the action of a varying-with-angle load. The same experiment carried out in section 6.1.2 will be done for the new specimen. The results are given in the following chart.

α (°)	Critical Load (MPa)
30	701,7640984
60	631,4884401
90	609,1661408
120	598,650393
150	592,7671964
180	589,1256956
210	586,7147611
240	585,0324135
270	583,7953933
300	582,824422
330	581,9631691
360	579,3607653

Chart 6: Critical load as a function of the triangularly distributed load's slope

In the next diagram, the critical loads of both cylinders with constant and variable section of wall are compared. As it could be expected, the thickness increase on the bottom of the shell makes it more stable than the one with constant wall. A remarkable fact lays in the middle of the diagram. While in the cylinder with constant section the critical load fell down in the middle values of the load applied angle, the new cylinder is not only more stable itself, but much more stable for the angles between 90° and 330°.

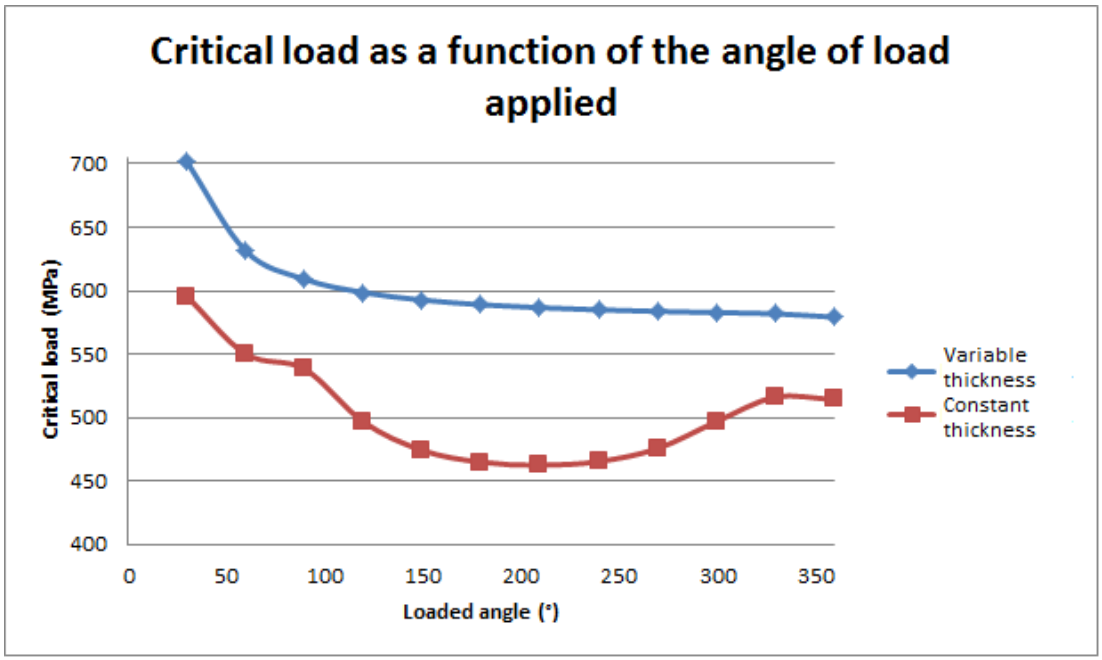

Diagram 7: Critical load as a function of the angle of load applied

To see the effects of the wall variation on the cylindrical deformed shape, models subjected to uniform axial load (360°) are plotted.

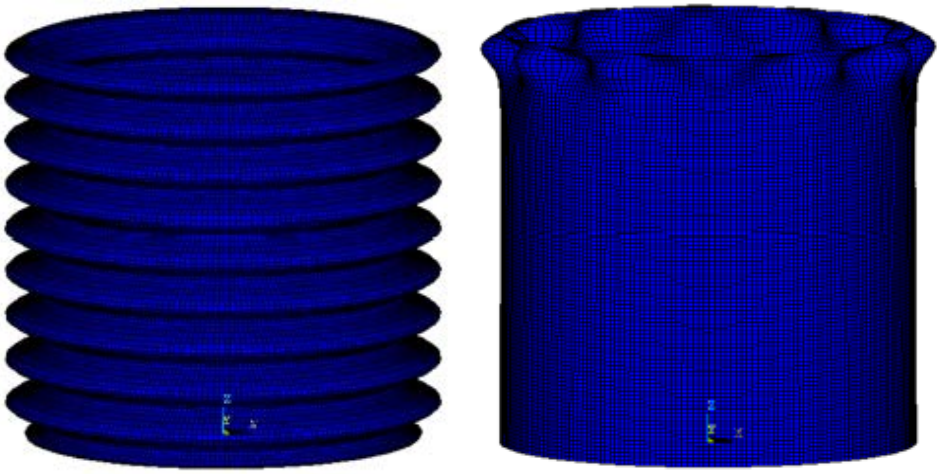

Figure 38: Behavior of the model with constant thickness wall (left) and variable thickness wall (right).

As the figures depict, variable thickness along the wall does not only affect to the critical load needed to buckle, but also to the shape of the cylinder after it: the new cylinder is much more stable.

6.2.3 Buckling analysis of a cylindrical shell with variable section under triangularly distributed axial load.

The cylindrical shell with variable section will be now subjected to triangularly distributed load. The results are presented in the next chart.

Slope (kN/°)	Maximum load applied (kN)	Critical load(MPa)
0,02	3,6	2819,86
0,1	18	698,632
0,2	36	360,026
0,4	72	182,8152
0,6	288	122,5124
0,8	144	92,1244
1	180	73,8152
1,5	270	49,3134
2	360	37,024
2,5	420	29,6378

Chart 7: Critical load as a function of the triangularly distributed load's slope (or maximum load applied)

In the next diagram, the results of this and the constant wall tests are compared.

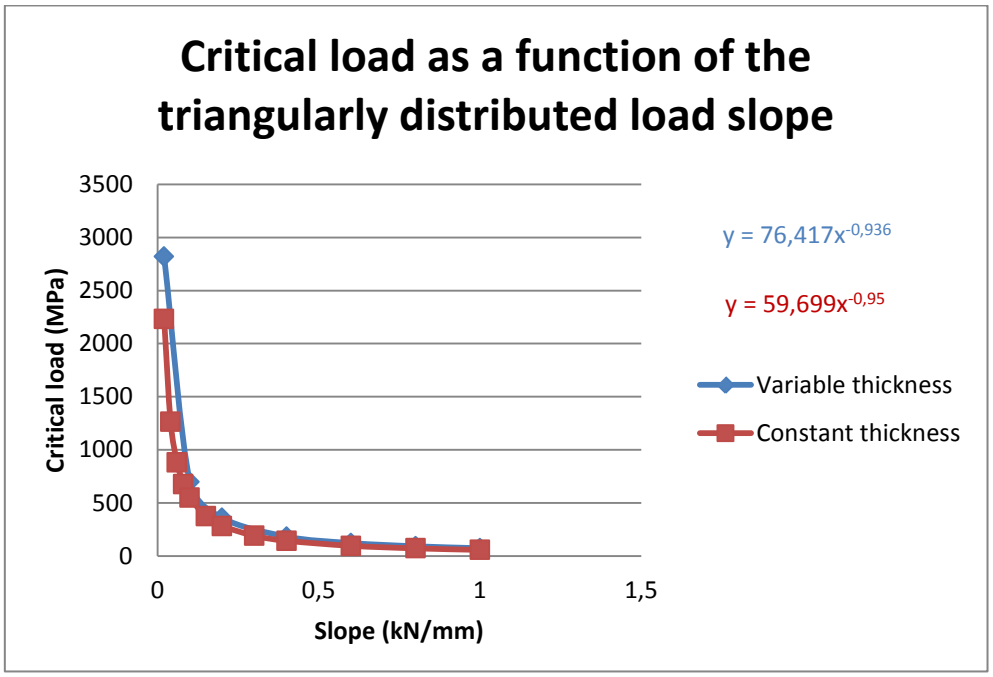

Diagram 8: Critical load as a function of the slope of triangularly distributed load

The data can be almost perfectly adjusted by the power equations above. Again, the cylinder with variable wall is more stable, having a critical load approximately 20% bigger. The functions can be used to predict the behavior of both models for different slopes of triangularly distributed load applied axially.

7. LINEAR STABILITY ANALYSIS OF CIRCULAR CYLINDRICAL SHELLS UNDER RADIAL LOAD

7.1 Analysis of perfect cylindrical shells under radial load

7.1.1 Introduction

In this section, the stability calculations using the finite element program ANSYS will be carried out under radial load.

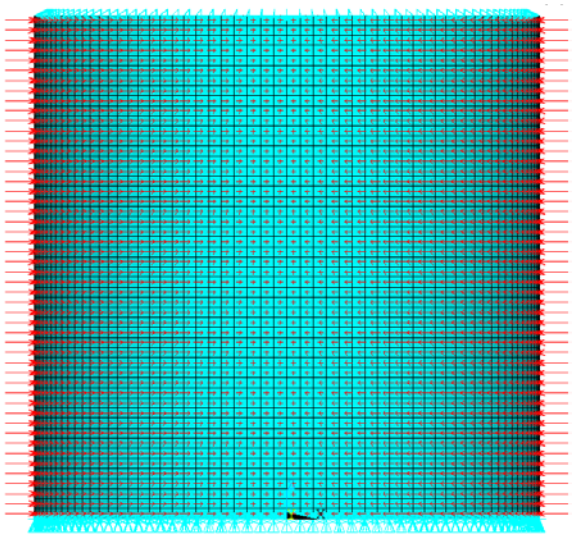

Figure 39: Model studied with ANSYS. Boundary conditions.

As in the axial case, the structure is supported at the bottom, restricting displacements in the three directions. In this case, the upper edge of the shell is only restricted in the radial direction. The load is applied in the radial direction. The initial phase of the investigation is carried out on a perfect cylindrical shell subjected to uniformly distributed load. Then the analytical solution is compared with the results calculated with ANSYS. In the course of this

chapter, different configurations of radial loads will be studied:

- Buckling analysis of cylindrical shell under uniform radial load.
- Buckling analysis of cylindrical shell under partial radial load.
- Buckling analysis of cylindrical shell under triangularly distributed radial load.

The referent material will be steel.

7.1.1.1. Specifications

The specifications are the same as the ones assumed in the axial tests. The only change will be the load that, in this case, will be applied in the radial direction.

7.1.1.2. Discretization and mesh. Validation of the model

For the validation of the model, Von Mises equation is utilized. It may be used for cylinders subject to combined radial and axial pressure, or just radial. The critical pressure is

$$\boldsymbol{P_C} = \frac{1}{n^2 - 1 + \left(\frac{\pi d}{8L}\right)^2}\left[\left(\left[n^2 + \left(\frac{\pi d}{2L}\right)^2\right]^2 - 2k_1 n^2 + k_2\right) * \frac{1}{3}\frac{2E}{1-\mu^2}\left(\frac{t}{d}\right)^3 + \frac{\frac{2Et}{d}}{\left[\left(\frac{2nL}{\pi d}\right)^2 + 1\right]^2}\right]$$

$$= \boldsymbol{0,1090506\ MPa}$$

where

$$k_1 = (1 + (1+\mu)\rho)(2 + (1-\mu)\rho) = 2{,}16267$$

$$k_2 = [1 - \rho\mu]\left[1 + \rho(1+2\mu) - \mu^2(1-\mu^2)\left(1 + \frac{1+\mu}{1-\mu}\rho\right)\right] = 0{,}961026$$

and

$$\rho = \frac{1}{\left(\frac{2nL}{\pi d}\right)^2 + 1} = 0{,}037122$$

The solutions obtained with ANSYS are represented in the following figures.

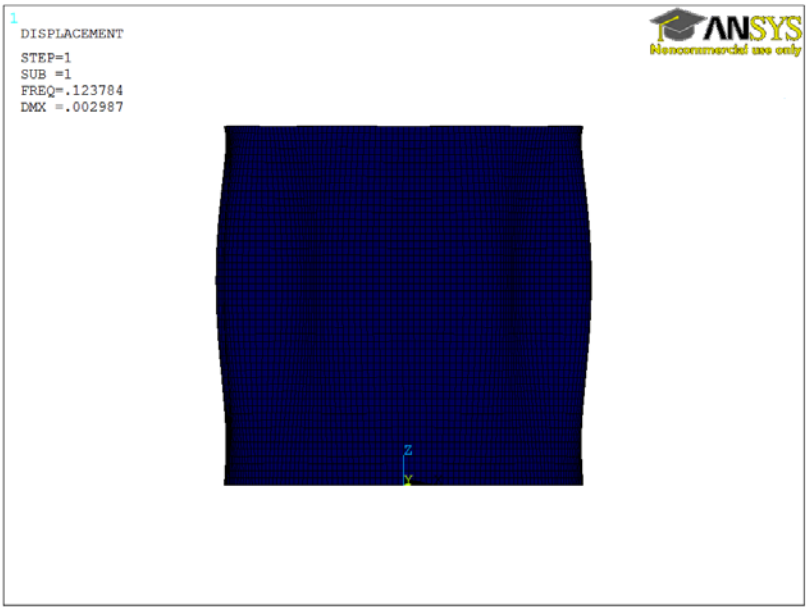

Figure 40: Solution with Shell-63

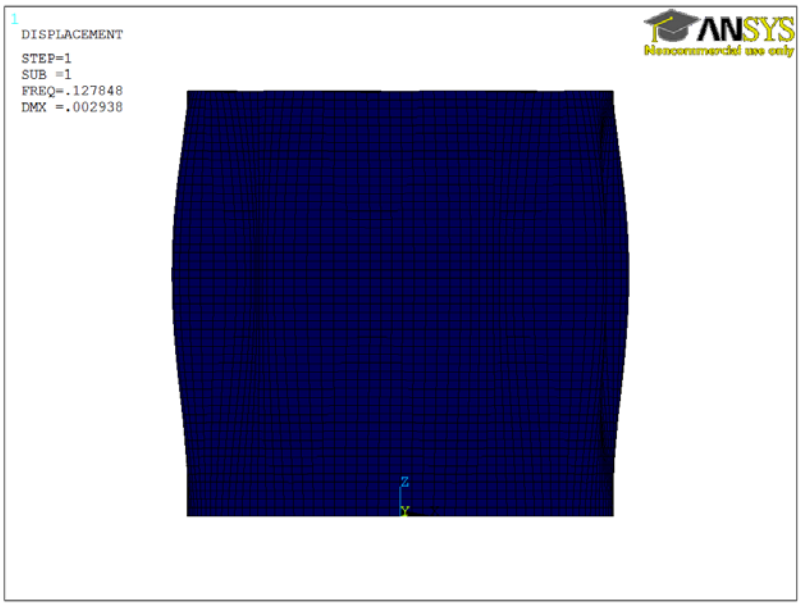

Figure 41: Solution with Solid-45.

It can be observed that the results obtained with ANSYS approximate the analytical solution, with a deviation of 11,4 % for Shell-63 and 14,2 % for Solid-45.

7.1.2. Buckling analysis of a perfect cylindrical shell under partial radial load, using Shell-63 and Solid-45.

At this point, the behavior of the model subjected to different angles of load will be analyzed. The test will be carried out with a load of 1 MPa.

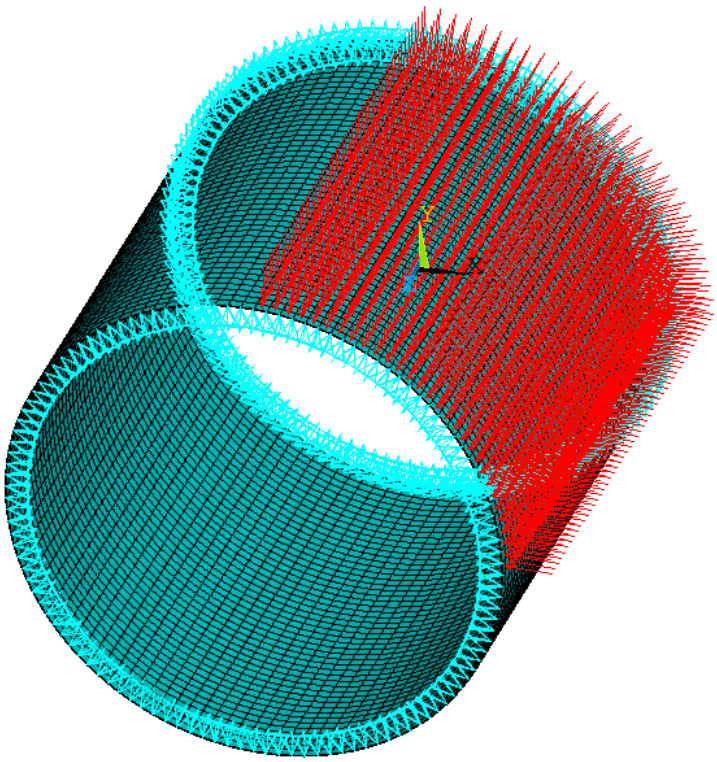

Figure 42: Model under 90^0 radial compression

Angle of application (°)	Critical load Solid 45 (MPa)	Critical load Shell 63 (MPa)
30	0,22939233	0,21936308
60	0,16349204	0,15485509
90	0,14859745	0,14154763
120	0,1412661	0,13527128
150	0,13721042	0,13155564
180	0,13268571	0,12928574
210	0,13299288	0,12786457
240	0,1318177	0,12679832
270	0,13093318	0,12600647
300	0,13022667	0,12541804
330	0,12956091	0,12488341
360	0,12784779	0,12378428

Chart 8: Critical load as a function of the angle of load applied, with Solid-45 and Shell-63

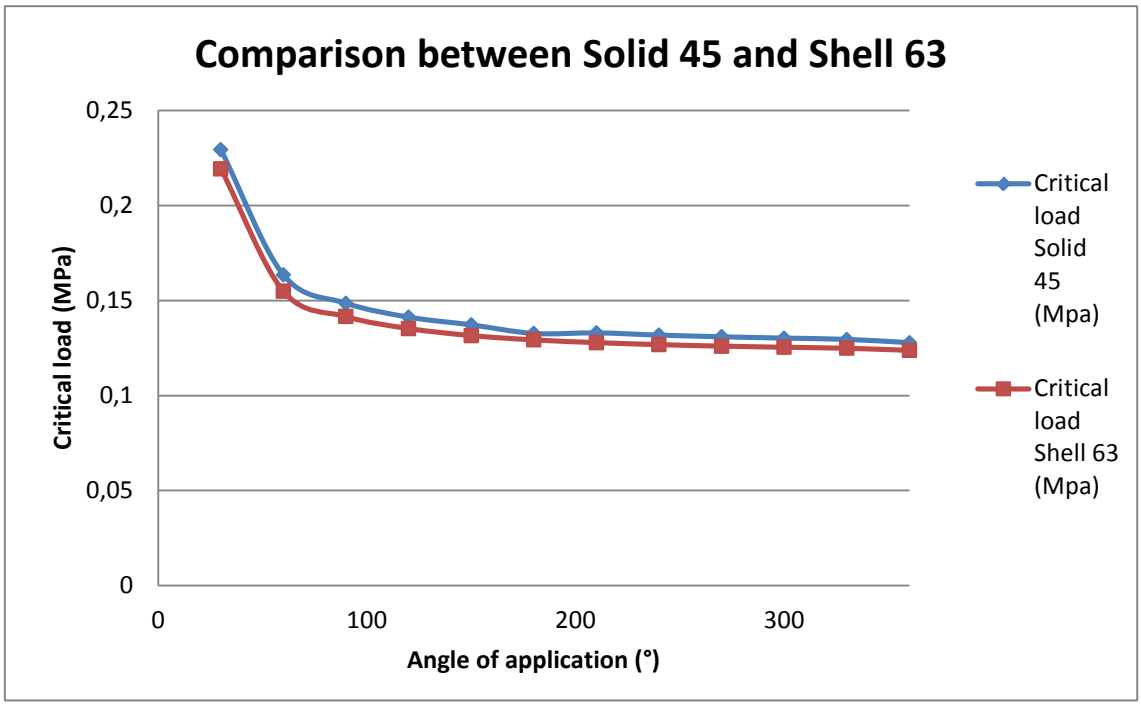

Diagram 9: Critical load as a function of the angle of load applied, with Solid-45 and Shell-63

As the diagram indicates, the critical load drops when increasing the area on which the pressure is applied. The following graphs present how the model is deformed when applying loads at a quarter, a half, three quarters and the whole cylindrical area.

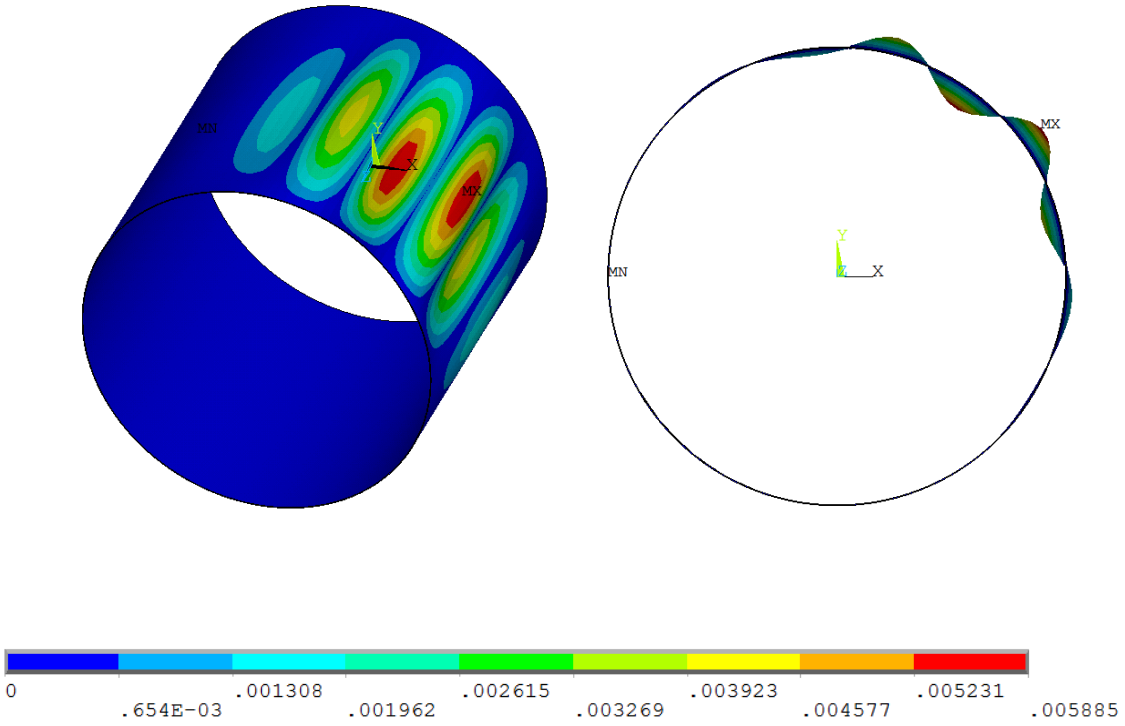

Figure 43: Deformed model after applying 90^0 radial compression

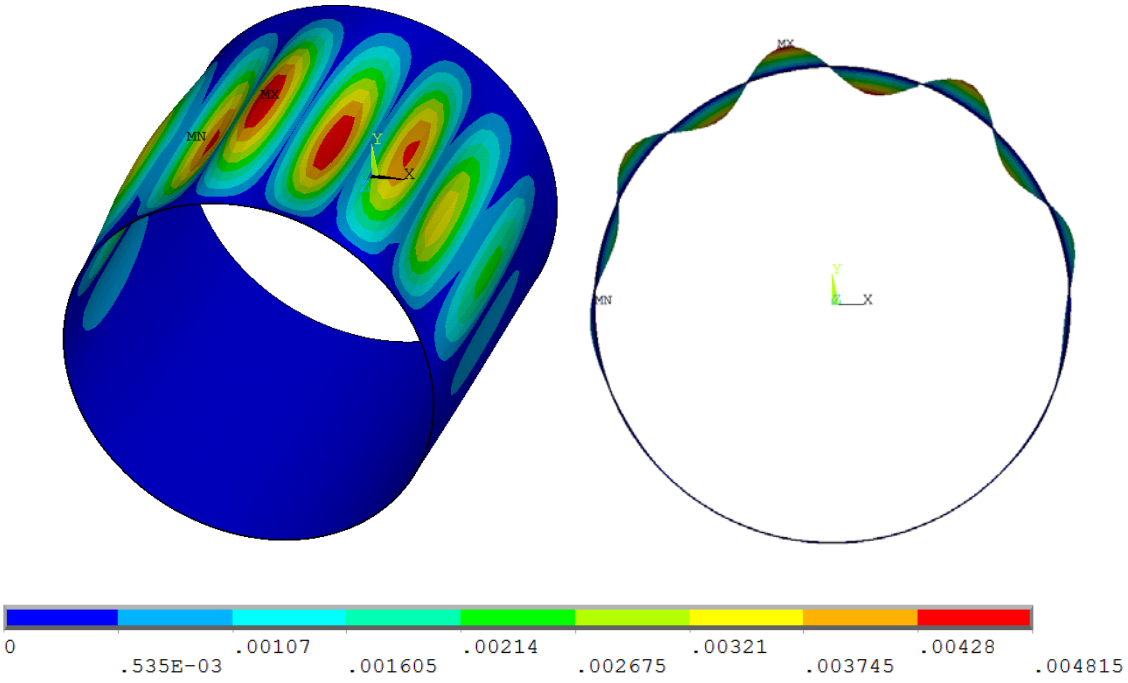

Figure 44: Deformed model after applying 180^0 radial compression

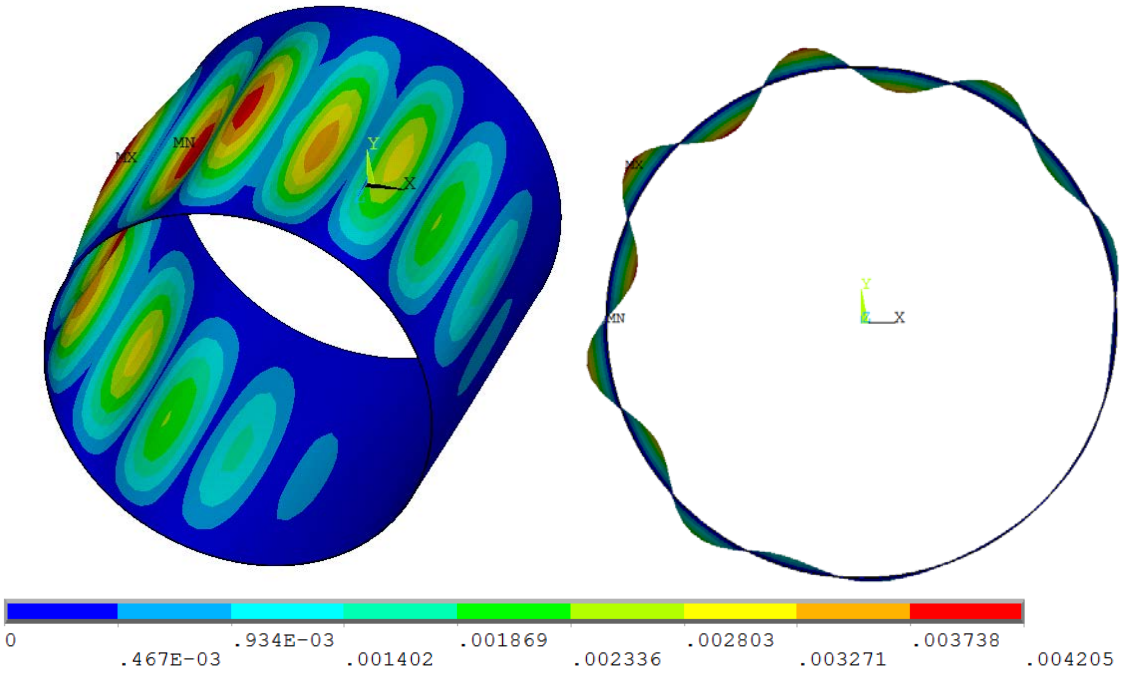

Figure 45: Deformed model after applying 270^0 radial compression

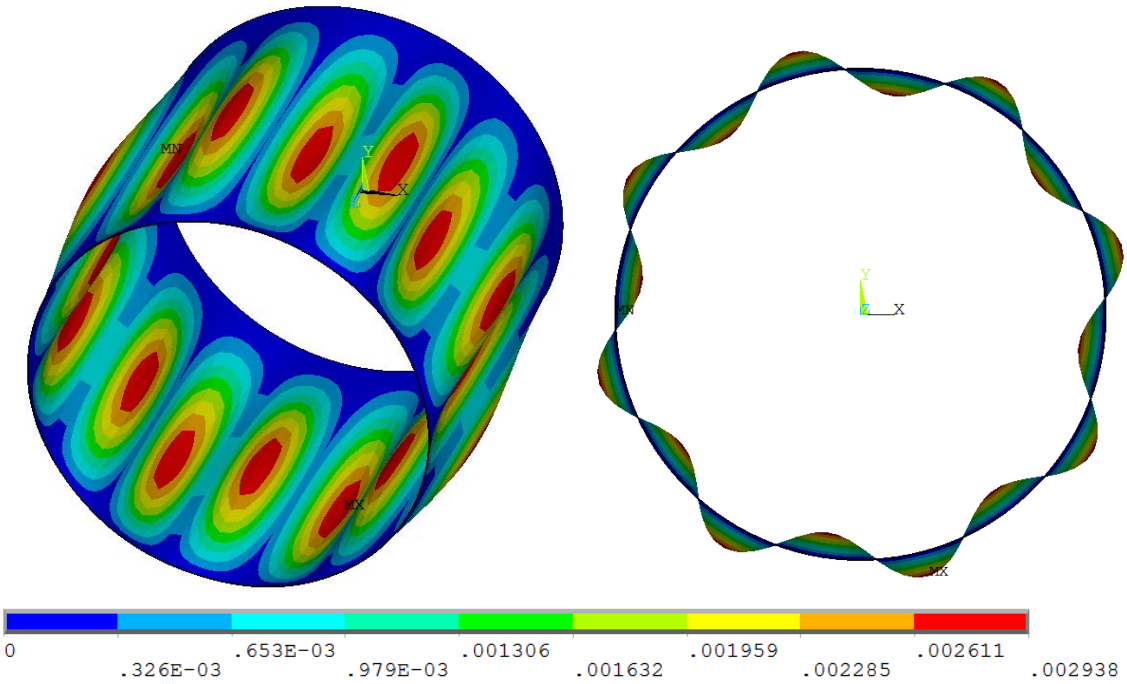

Figure 46: Deformed model after applying 360^0 radial compression

7.1.3. Buckling analysis of a perfect cylindrical shell under triangularly distributed radial load.

In this section, the cylinder will be subjected to a triangularly varying load. The model will be subjected to different values of load, in order to be able to predict how it would behave for any distribution of triangular load. Next plots represent the distribution applied on the cylinder and the section after buckling.

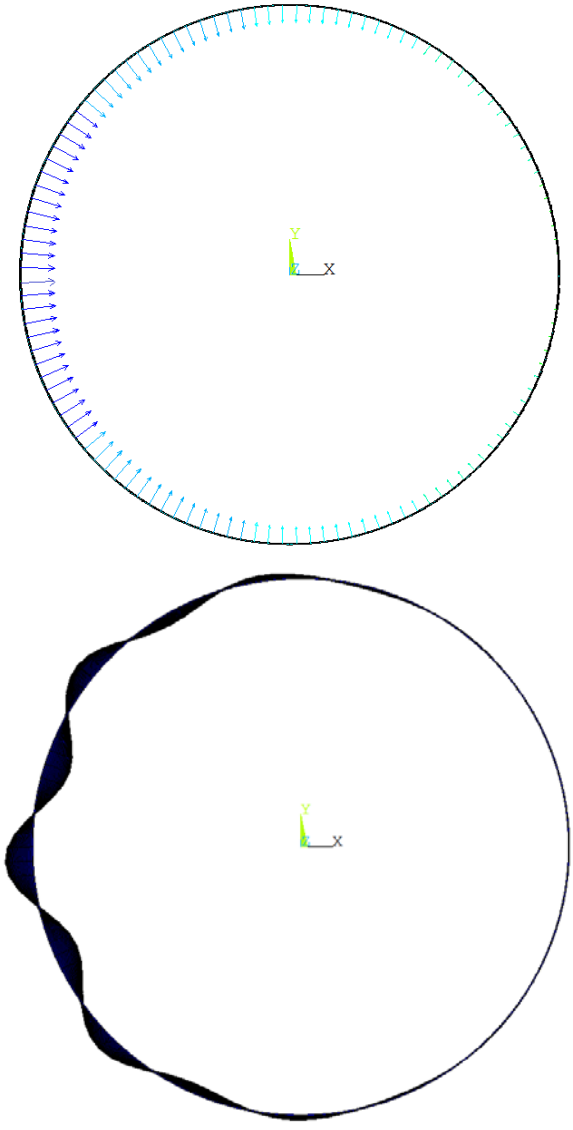

Figure 47: Triangularly distributed radial load applied and deformed shape after buckling

This table presents the data obtained after tests.

Slope (MPa/°)	Maximum value of the load (MPa)	Critical load (MPa)
0,0055555	1	0,146782
0,01	1,8	0,099653
0,02	3,6	0,068963
0,04	7,2	0,027554
0,06	10,8	0,017211
0,08	14,4	0,012513
0,1	18	0,009829
0,2	36	0,004743
0,3	54	0,003126
0,4	72	0,002331
0,5	90	0,001858
0,6	108	0,001545
0,7	126	0,001397
0,8	144	0,001156
0,9	162	0,001054
1	180	0,000923

Chart 9: Critical load as a function of the triangularly distributed load's slope (or maximum load applied)

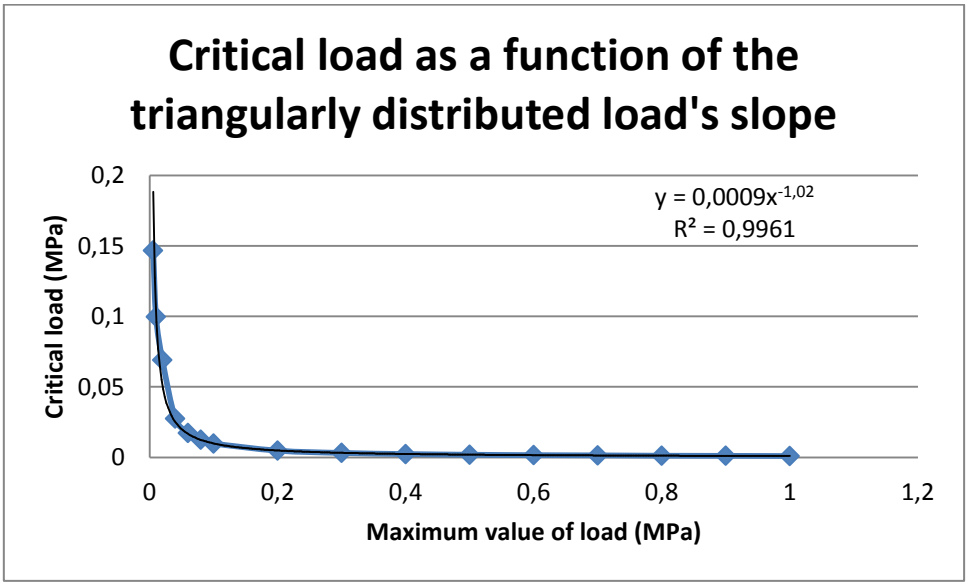

Diagram 10: Critical load as a function of the triangularly distributed load's slope

In the graphic above, the data are approximated by the equation $y = 0{,}0009x^{-1{,}02}$, which can be used to predict an approximate value of the critical buckling load for different values of the slope of the triangularly distributed load.

7.1.4. Buckling analysis of a perfect cylindrical shell under wind load.

In this part, the behavior of the cylinder under a model of wind load will be study. The wind load is simulated as follows: One half of the cylinder is subjected to external compression (where the wind comes into contact with the cylindrical shell), and the other one to internal compression (from where the wind leaves the cylinder). Both loads are triangularly distributed, having their maximum in the point where the wind is perpendicular. This patron of loading is taken from the part of wind loads of the German norm DIN 1055-4. The after coming figure represents this wind load.

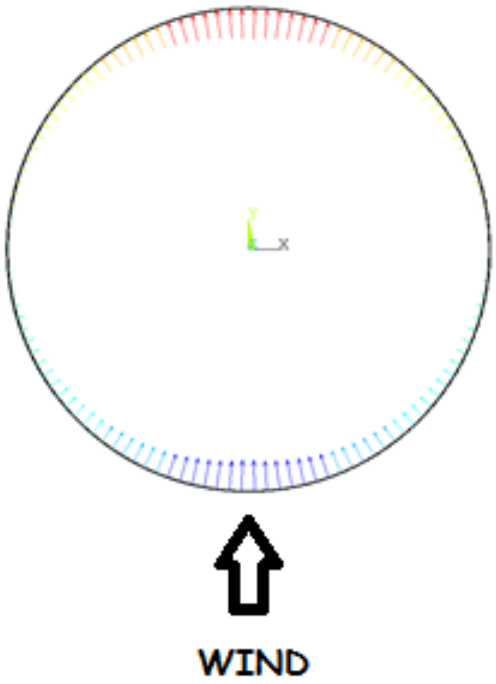

Figure 48: Model of wind

In the following chart, the results obtained from the simulations are written.

Slope (MPa/°)	Maximum value of load applied(MPa)	Critical load (MPa)
0,01111111	1	0,107099
0,111111111	10	0,023872
1	90	0,003905
2	180	0,001527
3	270	0,001018
4	360	0,000764
5	450	0,000611
6	540	0,000509
7	630	0,000487
8	720	0,000432
9	810	0,000397
10	900	0,0003055

Chart 10: Critical load as a function of the load's slope or maximum value of wind load

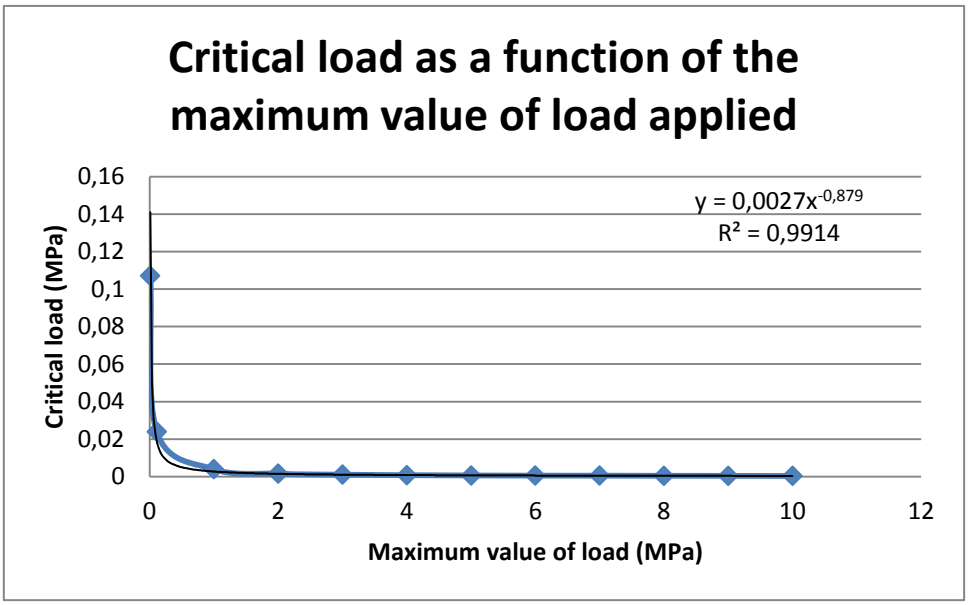

Diagram 11: Critical load as a function of the maximum value of load applied

From the diagram can be obtained an equation to approximate the critical load as a function of the maximum value of load applied, that is: $y = 0{,}0027x^{-0{,}879}$. The next figures represent de buckling deformation pattern of the cylinder under wind load.

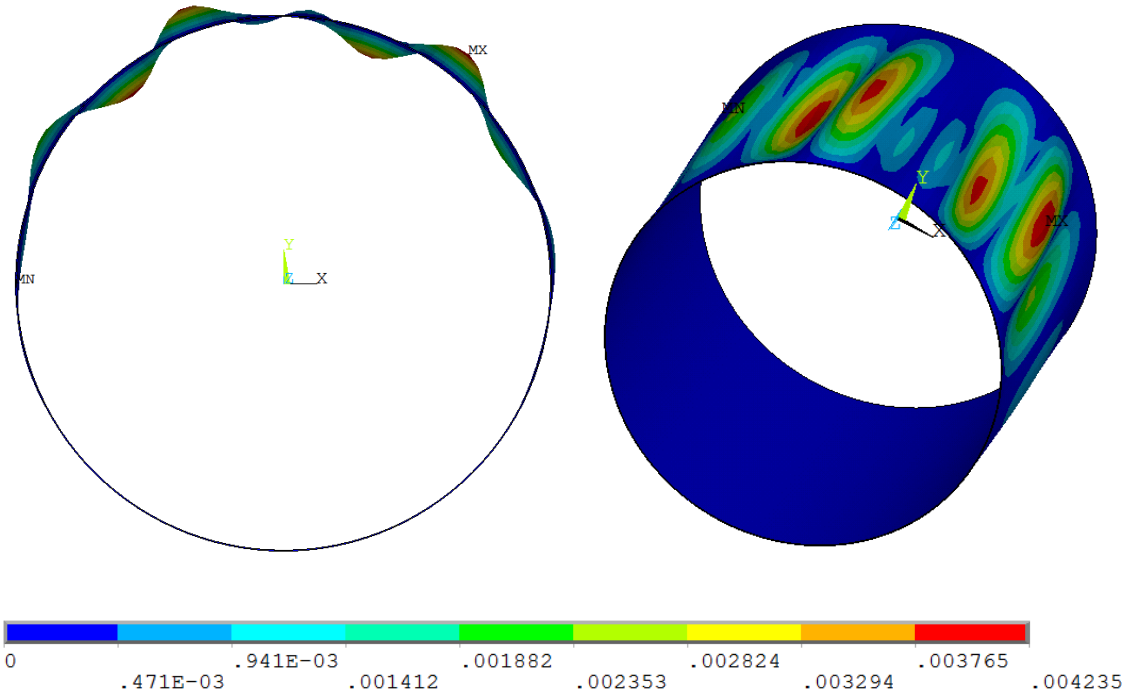

Figure 49: Wind loaded cylinder after buckling

7.2 Analysis of cylindrical shells with variable section under radial load

7.2.1. Introduction

In this section, the cylindrical shell with a gradual variation of thickness along the shell described in section 6.2.1 will be investigated under the action of several distributions of axial load.

7.2.2 Buckling analysis of a cylindrical shell with variable section under partial radial load.

At this point, the behavior of the cylindrical shell with variable section under various values of angles of radial load is study. The results are presented in the following table.

Angle (º)	Critical load (MPa)	Maximum displacement (mm)
30	0,322134	0,005729
60	0,2211	0,008781
90	0,21436	0,007533
120	0,210542	0,006638
150	0,208307	0,006235
180	0,206881	0,006049
210	0,20592	0,005815
240	0,205262	0,005485
270	0,204803	0,005336
300	0,20447	0,005108
330	0,20418	0,004841
360	0,203694	0,003132

Chart 11: Critical load and maximum displacement as a function of the load's angle

Now, the results for the experiment with constant and variable wall thickness are compared.

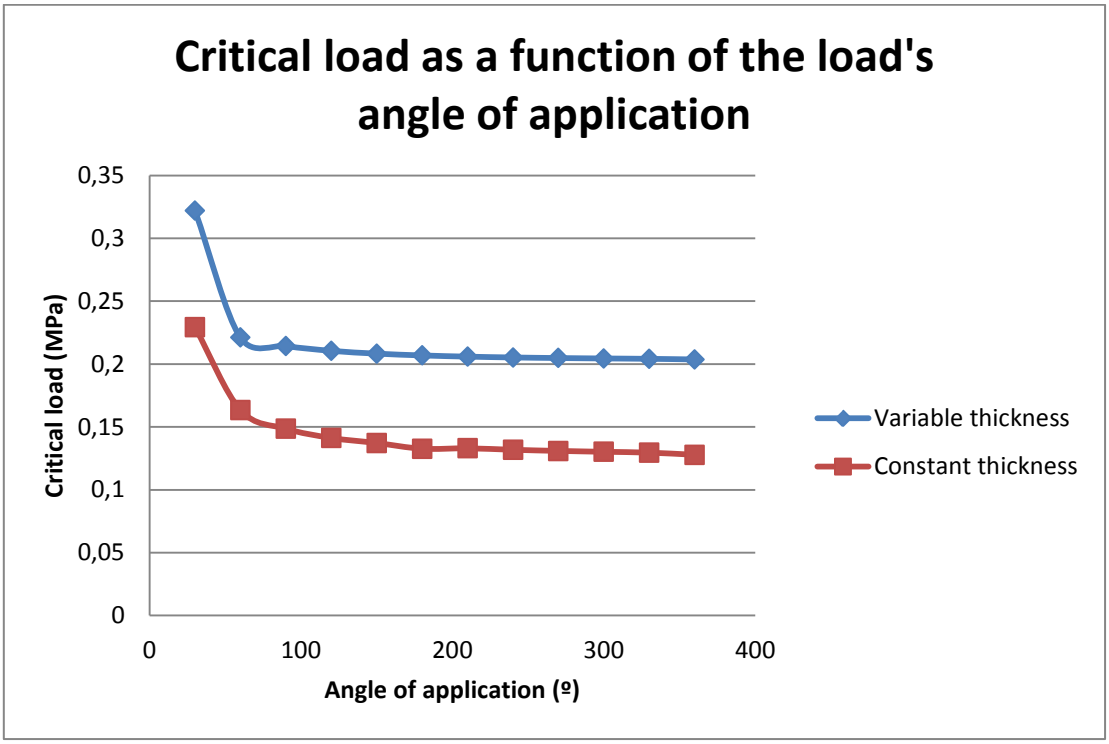

Diagram 12: Critical load as a function of the load's angle of application for variable and constant thickness wall

One can see that the cylinder becomes between 20-30% more stable when the bottom part of the cylinder is doubled. However, both of them follow the same downward trend.

7.2.3 Buckling analysis of a cylindrical shell with variable section under triangularly distributed radial load.

In this section, the triangularly distributed load will be applied on the model. The result after buckling is presented in the following image.

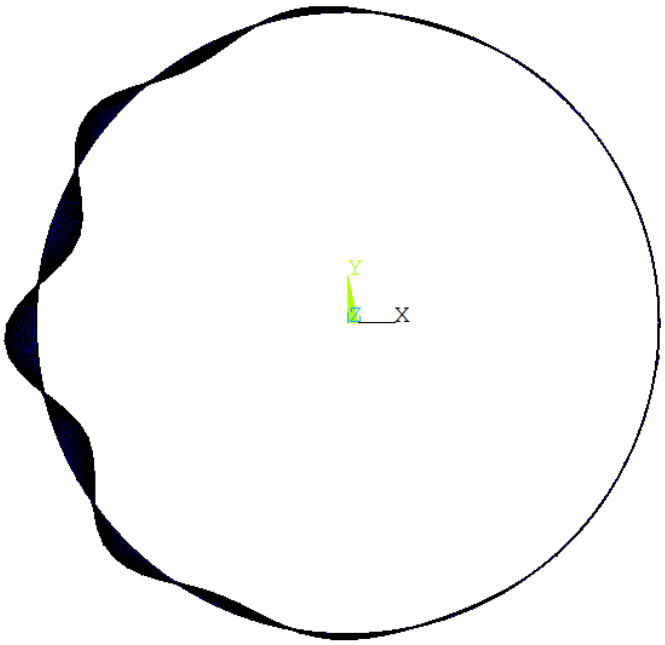

Figure 49: Shape of the model after buckling under triangularly distributed radial load

Slope (MPa/^{0})	Maximum value of load (MPa)	Critical load (MPa)
0,005555556	1	0,559375
0,02	3,6	0,163306
0,04	7,2	0,065196
0,06	10,8	0,040715
0,08	14,4	0,03158
0,1	18	0,02325
0,2	36	0,011219
0,3	54	0,00784
0,4	72	0,005513
0,5	90	0,004395
0,6	108	0,003654
0,7	126	0,003075
0,8	144	0,002733
0,9	162	0,002512
1	180	0,002183

Chart 12: Critical load as a function of the slope of the triangularly distributed load

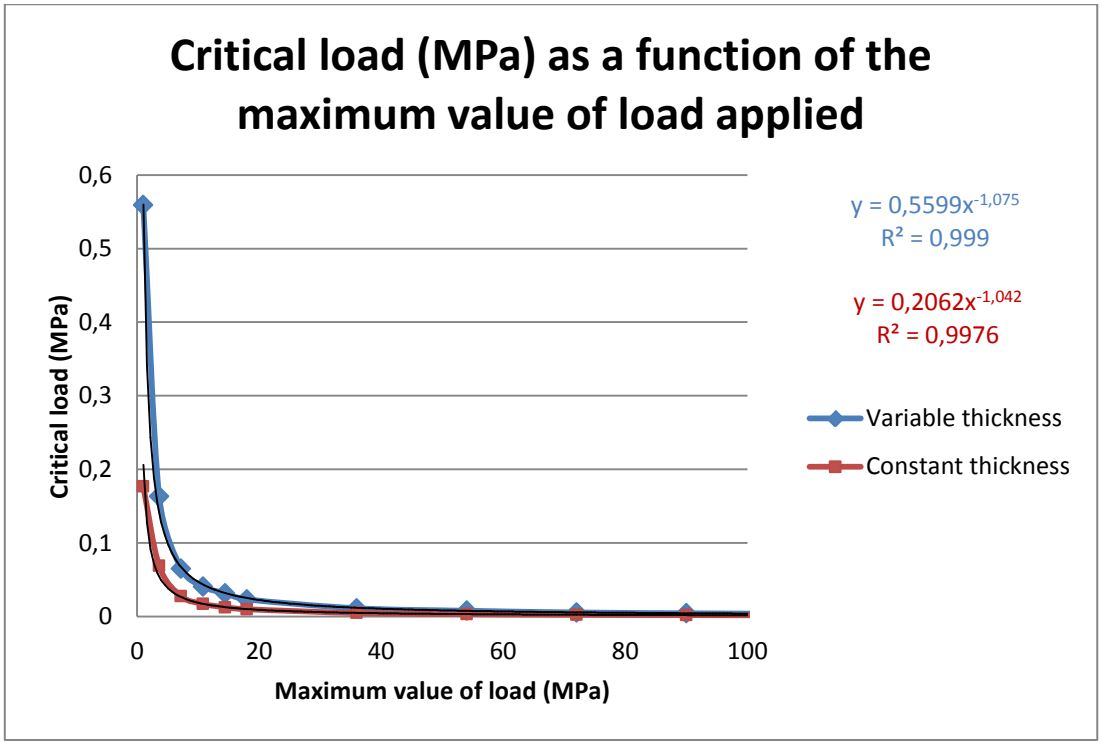

Diagram 13: Critical load as a function of the load's angle of application for variable and constant thickness wall

Diagram 13 depicts the critical buckling load for both models under study. Again, as expected, the cylinder with variable thickness wall is more stable. The equations written on it can be used to predict the critical load for any value of the triangularly distributed load's slope.

7.2.4 Buckling analysis of a cylindrical shell with variable section under wind load.

In the last section, the behavior of the variable wall specimen under wind load will be examined. Several sets of wind load are introduced into the ANSYS program, in order to obtain a trend for the cylindrical shell's response to the different wind forces.

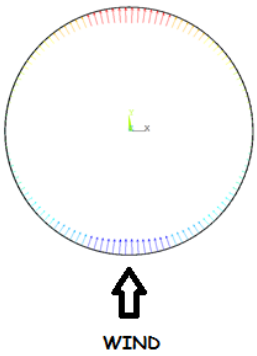

Figure 50: Model of wind

The succeeding data represent the response of the cylinder to different slopes of the wind load simulation.

Slope (MPa/°)	Maximum value of load (MPa)	Critical load (MPa)
0,011111111	1	0,3557
0,111111111	10	0,035493
0,5	45	0,012924
1	90	0,006483
2	180	0,003242
3	270	0,002161
4	360	0,001621
5	450	0,001346
6	540	0,001098
7	630	0,000967
8	720	0,000883
9	810	0,000796
10	900	0,000756

Chart 13: Critical load as a function of the slope of the wind load or its maximum value

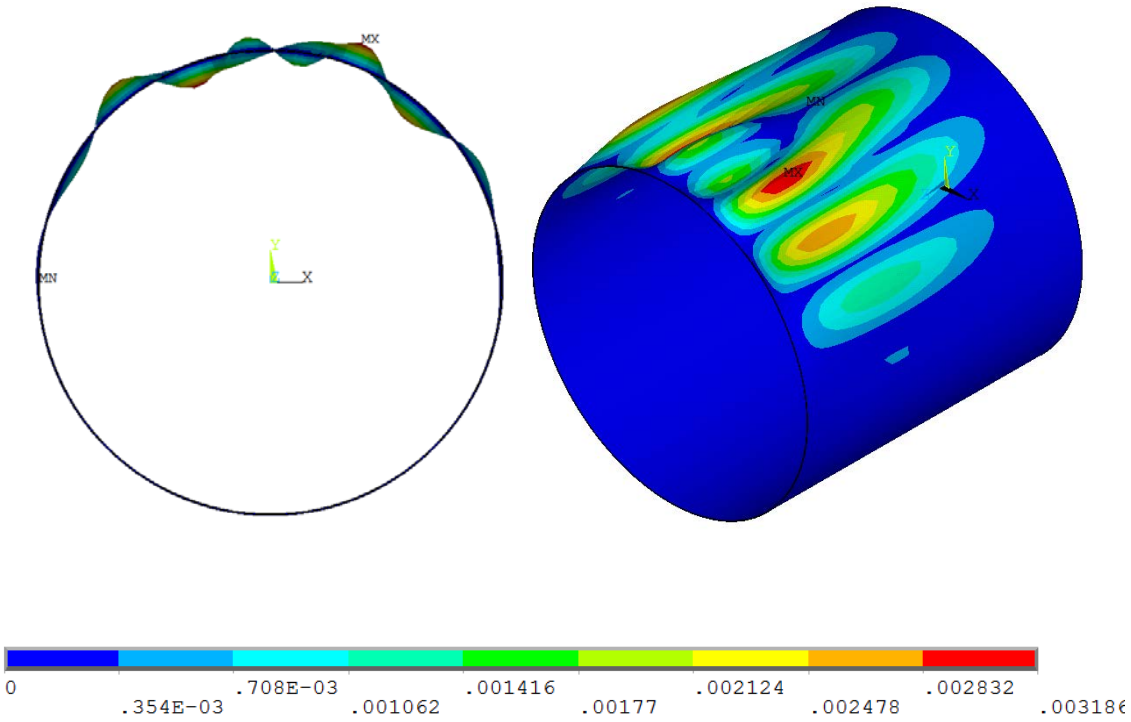

Figure 51: Deformed shape when applying the model of wind load (slope 1 MPa/^{0})

The figures above depict the deformation's pattern of the cylinder after buckling. There are a few details to stand out in both displacement figures.

The displacement are concentrated in just one half of the shell, the part from where the wind leaves the cylinder. Moreover, the varying thickness of wall is obvious, and there do not exist deformations in the bottom part of the shell.

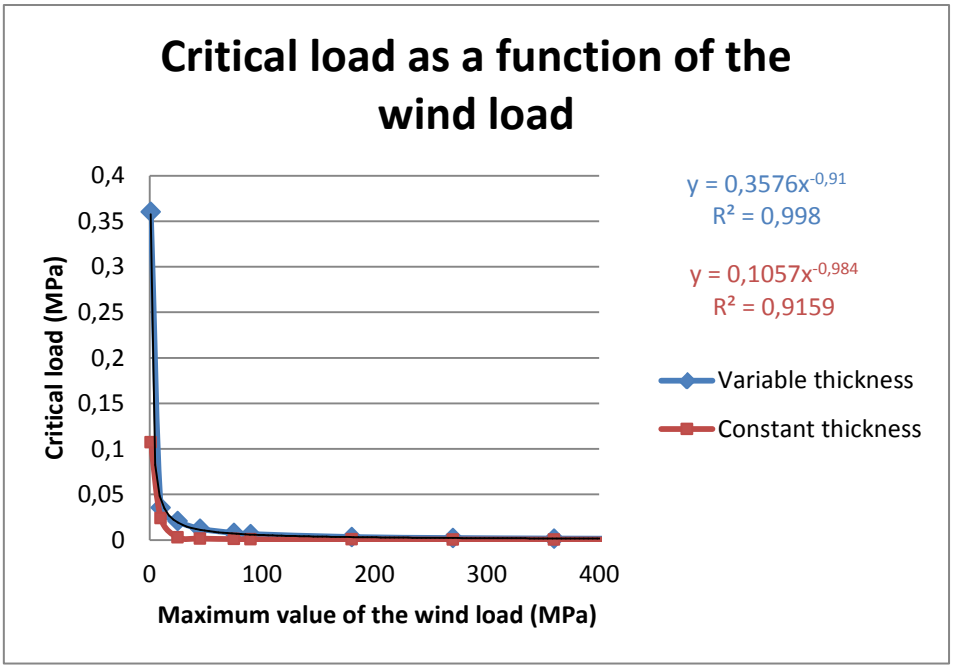

Diagram 14: Critical load as a function of the maximum value of wind load

The graphic above shows the difference that produces increasing the bottom part of the former cylindrical shell to the double.

Moreover, the equations displayed could be used to predict an approximate value of the critical buckling load under any maximum value of wind load applied.

8. CONCLUSIONS

The basic idea of this thesis was to discuss the influence of different load distributions (uniform, partial, triangularly distributed) have in the value of the critical buckling load of cylindrical shells, both axially and radialy applied. The cases were analyzed using the Finite Element Method.

In order to achieve that aim, also different section configurations have been analyzed. That has provided information about the buckling behavior of cylinders subjected to various types of load, such as the wind load model. There has been found out how a cylindrical shell behaves under unirform and non-uniform loads. Since there are not many researches on the field of cylinders subjected to non-uniform loads, the results obtained can be interesting to predict how cylindrical shells might buckle under the load distributions that ave been examined.

Because of my interest in the field of finite element analysis, I have decided to deepen my knowledge in this area through this thesis. In this thesis, I have succeeded in this area further training and to integrate the measurement program ANSYS with success.

The skills learned are a good foundation for my career to become a design engineer.

9. BIBLIOGRAPHY

[1] ELLER, C.: Finite–Elemente–Methode der Statik und Dynamik, Vorlesungsskript, Hochschule Niederrhein, Krefeld 2011.

[2] X.WANG, JUN XIAO, Y.C. ZHANG: A method for solving the buckling problem of a thin-walled shell.

[3] ANSYS online help.

[4] CARNICERO A.: Introducción al método de los elementos finitos.

[5] "Meet the Finite Element Method", PDF Format, available in "media.wiley.com/product.../0471370789.pdf"

[6] SEUNG-EOCK KIM, CHANG-SUNG KIM: Buckling strength of the cylindrical shell and tank subjected to axially compressive loads

[7] C.Y. SONG, J.G. TENG, J.M. ROTTER: Imperfection sensitivity of thin elastic cylindrical shells subject to partial axial compression

[8] DANIEL VASILIKIS, SPYROS A. KARAMANOS: Stability of confined thin-walled steel cylinders under external pressure.

[9] DIRK PONS: Structural Mechanics, Third edition 2010.

[10] LESLIE K. GUICE, J.Y.Li: Buckling Models and Influencing Factors for Pipe Rehabilitation Design.

[11] UNIVERSITY OF LJUBLANA: Applied Stability.

[12] PLYMOUTH UNIVERSITY: Stresses in cylinders and spheres.

[13] GEORGE S J SIMITSES: Buckling and postbuckling of imperfect cylindrical shells: A review.

[14] HUTCHINSON, J.W., KOITER, W.T.: Postbuckling Theory.

[15] B.PRABU, A.V.RAVIPRAKASH, N.RATHINAM: Parametric study on buckling behaviour of thin stainless steel cylindrical shells for circular dent dimensional variations under uniform axial compression.

[16] VASILI TOROPOV: Theory and methods for evaluation of elastic critical buckling load.

[17] EUROCODES.

[18] GODOY, A.LUIS; FLORES, FERNANDO G.:Imperfection sensitivity to elastic buckling of wind loaded open cylindrical tanks